

2.017 Design of Electromechanical Robotics Systems

Retrieval of Ghost Lobster Pots using ROVs Final Report

by

River Adkins, Jack Dirig, Thao Do, Kelsey Fontenot, Ved Ganesh,
Matthew Kim, Gage Lankford, Teagan Sullivan, Amir White

MASSACHUSETTS INSTITUTE OF TECHNOLOGY
5/14/2025

Abstract	3
I. Introduction & Background	3
II. System Overview	6
III. Localization	8
A. USBL Range & Accuracy Testing	10
B. Potential Failure Modes	18
IV. Navigation	19
A. Communication Protocol	20
B. Driving Process	21
C. Testing	22
D. Issues and Debugging	24
E. Navigation Conclusions	25
V. Recovery	25
A. Overall Design Requirements	25
1. Surface Constraints:	26
2. Subsurface Constraints:	26
B. Tethered Connection	27
C. Engagement	29
D. Initial Prototype	33
E. Mechanical Fuse	35
1. Snap Shackle:	35
2. Shear Pin	36
F. Spear System Summary	44
VI. Integrated System	45
VII. Comparison to Current Solutions	49
VIII. Future Works	51
A. Localization	51
B. Navigation	52
C. Recovery	52
IX. Conclusions	55
References	57
Appendix	58

Abstract

Ghost lobster pots pose a significant threat to marine ecosystems since they continue to trap and kill marine life long after abandonment. Current retrieval methods are time-consuming, labor-intensive, and frequently environmentally damaging. To address these issues, a remotely operated vehicle (ROV) based retrieval system was developed that improves localization, navigation, and recovery of ghost pots. Our system integrates GPS-tagged sonar data, a USBL/DVL-based localization module, and autonomous waypoint navigation via QGroundControl to locate and move to the pot location. Once within six to eight meters of a tagged pot, the ROV uses onboard sonar and cameras to identify and latch onto the pot using a custom spear mechanism. Testing in the Zesiger Center pool and Charles River demonstrated the system's ability to reliably locate and retrieve pots with improved accuracy and reduced effort compared to traditional methods. This approach offers a scalable, cost-effective solution for mitigating ghost gear impacts and supporting sustainable lobster fisheries.

I. Introduction & Background

The 8.3 billion dollar lobster industry in the United States relies heavily on the use of lobster pots [1]. These wire cages sit on the seafloor and capture lobsters for later retrieval. They are connected to surface buoys with rope lines; when these lines detach or snap, pots are rendered irretrievable and become “ghost pots.” In Cape Cod alone, there are an estimated 12,500 to 33,000 lobsters killed per year due to ghost lobster pots [2]. With a market value of 30 dollars per lobster, this has large negative impacts on the lobster industry [3]. In addition to capturing and killing lobsters, the free-floating lines that remain connected to some pots entangle whales. Due to their negative impact on ocean habitat and the fishing industry, it is imperative

that abandoned pots are recovered or at least rendered incapable of continuing to trap and kill ocean life.



Fig. 1. Abandoned “ghost pot” on the seafloor [4].

While preventative methods—include redesigning gear to reduce the likelihood of failure, increasing navigational awareness by creating more distinct fisheries, reducing fishing effort, marking gear with GPS tags, and using biodegradable pots—have received increasing attention in recent years, they do not account for the millions of abandoned but still active lobster pots [5], [6].

Meanwhile, existing solutions for retrieving ghost pots are inadequate. One method, practiced by researchers at the Cornell Cooperative Extension, involves dragging 500 ft of grappling hook and cable across the ocean bottom, trawling for pots [7]. Researchers at the University of Delaware (UDel), meanwhile, are working on a more targeted retrieval method using side-scan sonar to detect and tag pots with their GPS coordinates for later retrieval. However, even with GPS guidance, it is difficult to locate and latch onto pots. Dr. Cameron Bodine, a researcher at the University of Delaware who is developing GPS tagging technology, estimates that the time to arrive at GPS coordinates is around two to five minutes, but the act of latching onto a ghost pot can take anywhere from 10 to 15 minutes not including recovery time,

which takes an additional three minutes. A lack of manpower also leads to delays, with some tagged pots sitting untouched for weeks after initial marking. While there is reason to believe that UDel’s detection and tagging software can be easily adapted to lobster pots, the same cannot be said for their process of manual retrieval. Crab pots are typically set in shallow waters of two or three meters; lobster pots, meanwhile, typically sit 30 to 100 meters below the surface, far too deep for a well-thrown grappling hook to latch on to with any reasonable confidence [8], [9]. An alternative method, more common to lobster pot retrieval, uses scuba divers for both tagging and retrieval [10]. However, the need for specialized skills, high equipment costs, and limited personnel caps the impact, as programs cannot extend past the amount of certified divers they have. Diver based methods recover pots at about a tenth the rate of trawling [7], [10].

To decrease the time to locate and latch onto tagged pots we implement an ROV-based retrieval method. Such a method promises to sidestep the canonical problems of low visibility and low resolution GPS coordinates that hinder current retrieval efforts.

II. System Overview

Our lobster pot retrieval process has three main stages: localization, navigation, and recovery (Fig. 2).

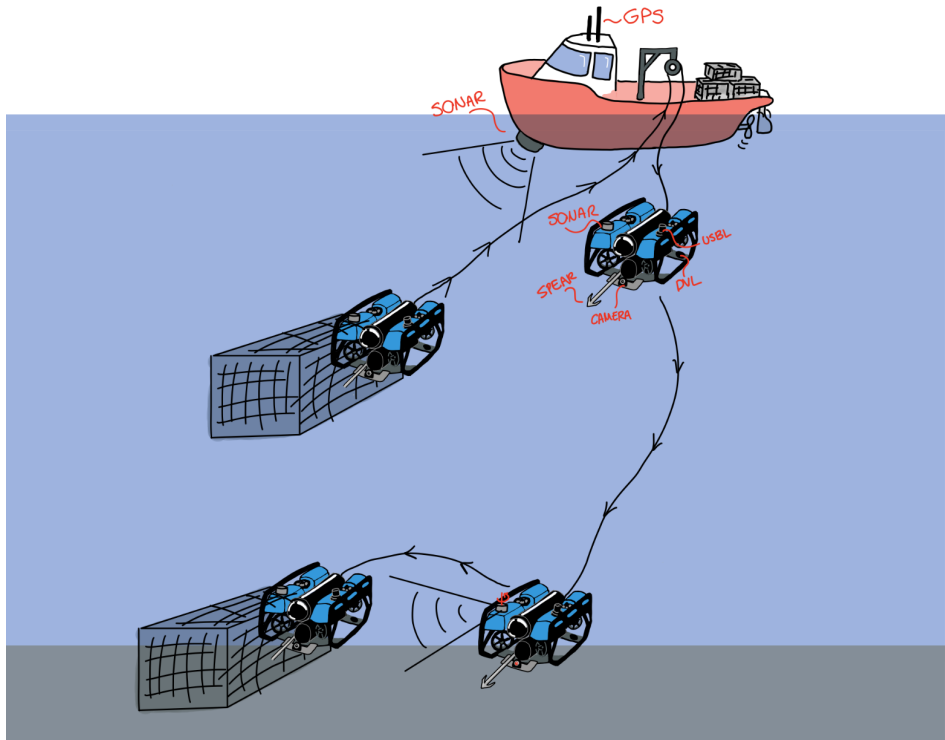


Fig. 2. Overview of ROV-based pot recovery system and process.

First, the operator uses the side sonar to scan the bottom of the body of water. This data is then fed into a software developed by UDel that analyzes the sonar data and outputs GPS locations of potential pots. The boat then navigates to the provided GPS coordinates. The user then deploys the ROV with the custom hook attachment and navigates the ROV to the exact pot GPS and depth given by UDel's software. This gets the ROV within eight meters of the true location of the pot. At this point, the user takes over manual control of the ROV, using the onboard sonar and camera to locate the lobster pot in the reference frame of the ROV. Once the pot is found, the user latches onto the pot using the hook. Upon successful engagement, the ROV is reeled in by its tether using the winch on board the boat. The pot can then be decoupled from the ROV by disengaging the hook, the ROV can then be rearmed, redeployed, and the process repeated.

Our retrieval system can be split into four main categories: surface modules, control, ROV, and hook (Fig. 3).

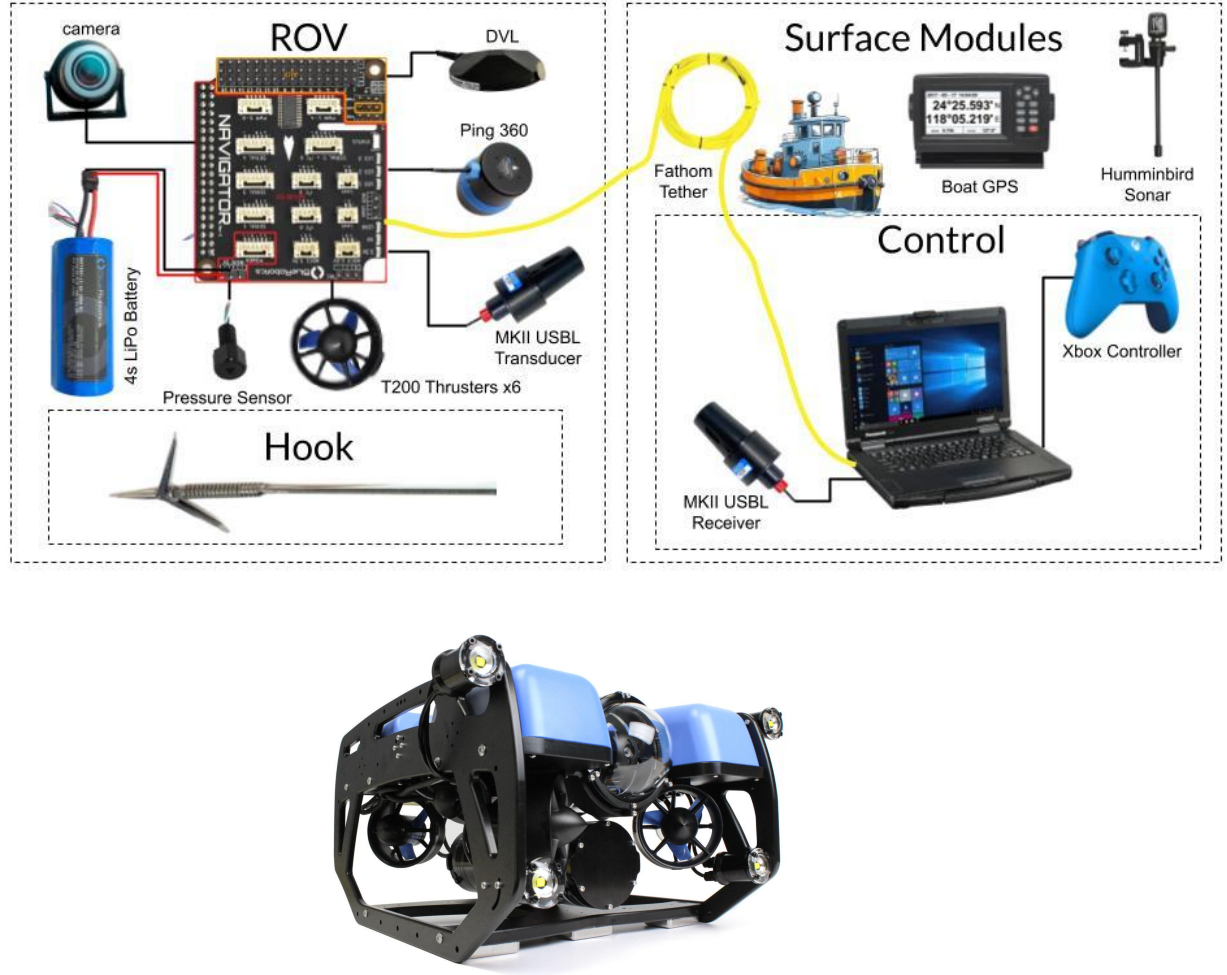


Fig. 3. Top: Modules and components of the ROV-based pot retrieval system. Bottom: The Blue ROV.

Our surface modules group consists of the boat or topside GPS, a Humminbird side scan sonar, the winch, and the boat itself. The control group includes the signal tether that connects to the ROV, the central control laptop, the MKII ultra-short baseline (USBL) receiver, and the joystick controller to drive the ROV. The ROV group consists of the essential ROV electronics, such as the flight controller, leak sensors, thrusters, pressure/depth sensors, and the battery, as well as an onboard Ping 360 sonar, a camera, a MKII USBL transceiver, and a Doppler velocity

logger (DVL). Finally, the hook category includes the barb, breakaway mechanism, and latch-box (last two not shown).

III. Localization

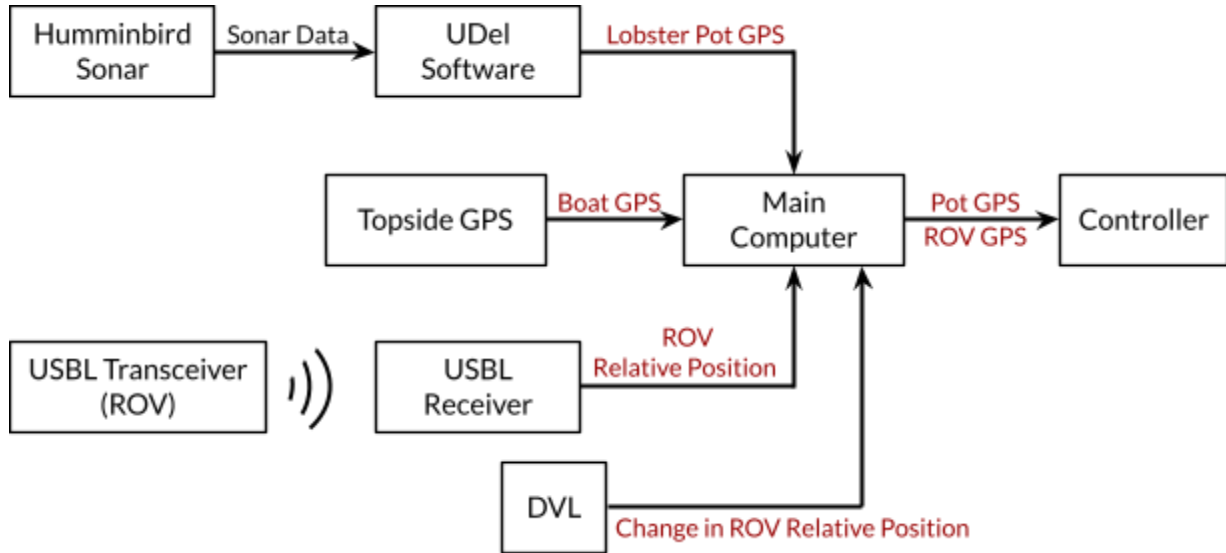


Fig. 4. Communication and data flow chart between system sensors to achieve pot and ROV GPS positioning in the real world.

The localization system must determine the live position of the ROV so that the ROV can be guided to the lobster pot using the GPS coordinates provided by the UDel software. To achieve this, our system utilizes a USBL and DVL to track the relative position between the boat/user and the ROV. The USBL receiver is attached to the boat while the transceiver is attached to the ROV. The two are synced, and from the direction and time it takes for the receiver to hear the clicks of the transceiver, a relative position of the ROV to the boat is calculated. The USBL update rate is 1 Hz. The DVL has four transducers emitting sound, which is then measured on return for each sound wave's Doppler shift. DVL update frequency is depth dependent, typically operating from 2 to 15 Hz. Using this, the DVL finds the relative velocity

of the ROV to the sea floor in three dimensions, allowing us to update our position information. Our relative position is then combined with DVL relative velocity to fine-tune our ROV position. The relative position is then converted to global coordinates using the GPS on the boat. The UDel system utilizes a side scan Humminbird sonar and can output GPS coordinates of lobster pots that are accurate to five meters horizontal distance. With the GPS of both the pot and the ROV known, the control system of the robot can then calculate the desired path and guide the ROV to the approximate location of the lobster pot.

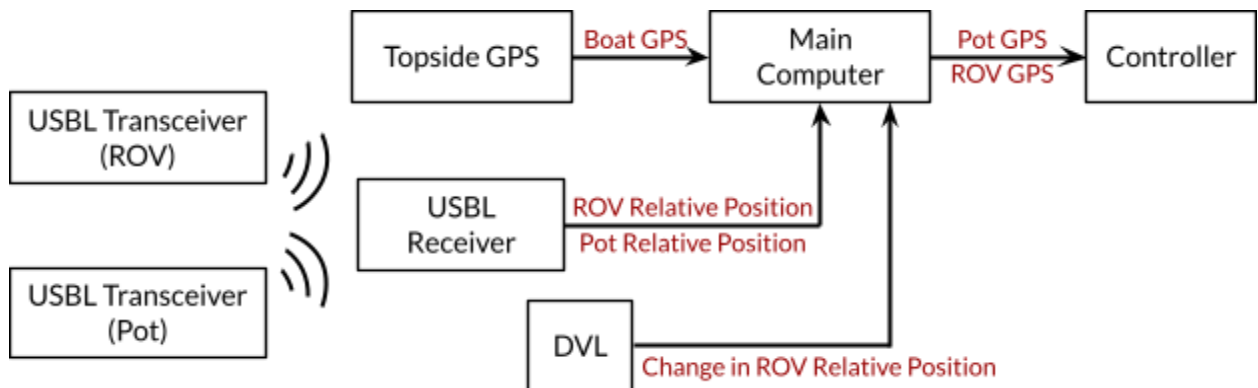


Fig. 5. Communication and data flow chart between system sensors to achieve pot and ROV GPS positioning in our testing environments.

Our real-world instrumentation setup is not ideal for the testing and development of our system. We made instrumentation substitutions to improve ease of development, while staying true to our expected real-world information. The UDel sonar system is intended for scanning whole bodies of water, then post-processing the data for later use to provide pot GPS and depth. This is not ideal for controlled live tests. A more accessible system is an additional USBL transmitter and hand-measured depth as a substitute. With this additional transmitter, we can track the live GPS coordinates of our test lobster pot using the same process as the ROV USBL, skipping the post-processing and scanning time. Additionally, in indoor environments, GPS accuracy suffers. Thus, rather than using a GPS unit like one you would find on a lobster boat, we spoofed our topside GPS to be a constant value. This should not negatively impact our

comparison, as our localization is purely relative to the boat GPS and should work the same for a non-fixed value.

A. USBL Range & Accuracy Testing

To confirm that the USBL is a suitable replacement for UDel-provided GPS coordinates and to assess the accuracy of the USBL position data, we conducted testing and data collection in a standard Olympic diving pool. By testing in a pool, we were able to measure the true distance, depth, and bearing of the lobster pot relative to the USBL receiver and compare it to the USBL output. However, testing in a pool also provides the most challenging environment for USBL accuracy due to the smooth, reflective environment. If the USBL performs well in our testing environment, the position tracking of the ROV in real-world environments, where acoustic reflection is less common, should only improve.

As shown in Fig. 6, the USBL receiver was located in the corner of the deepest end of the pool, while the USBL transceiver was located in the lobster pot. We recorded the depth, x-position, and y-position of the USBL transceiver and the lobster pot relative to the corner of the pool. Using this data, we calculated the true slant distance, bearing, and equivalent horizontal distance between the USBL receiver and the lobster pot. We also recorded the slant and bearing measurements output by the USBL system. These measurements were repeated for a total of four different lobster pot test positions.

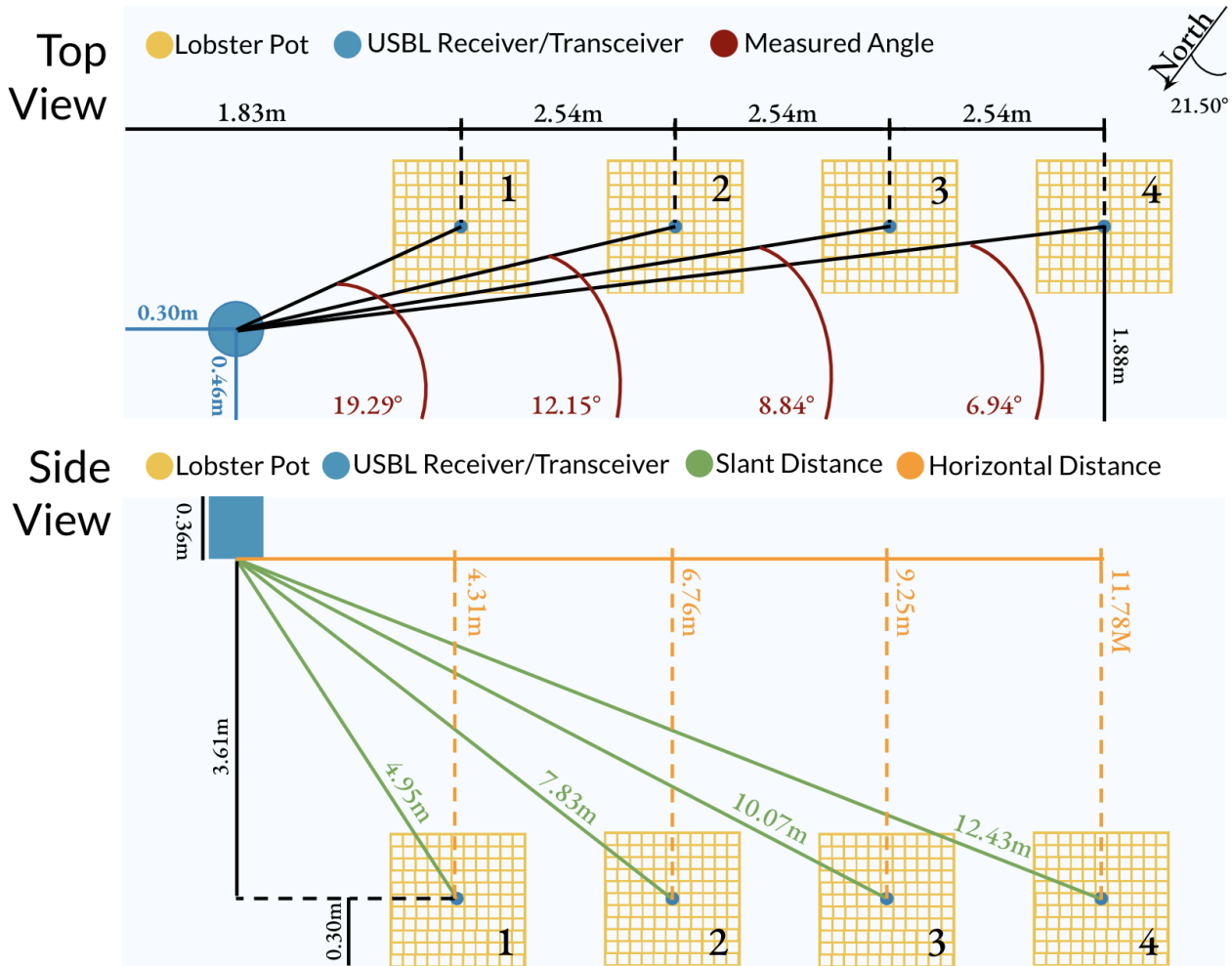


Fig. 6. USBL accuracy and range testing setup for diving pool testing. The true slant and bearing of the lobster pots were recorded and compared to the slant and bearing output by the USBL system.

We did not measure the Humminbird sonar accuracy as part of this testing, but instead relied on specifications from UDel that stated lobster pots could be located within 5 meters horizontally, and this is the number we will use for the following comparisons.

To verify that the USBL system is a suitable replacement for the UDel software, we converted the slant distance measurements to horizontal distance for a true comparison. We calculate horizontal distance from the slant distance and depth by using the Pythagorean theorem.

$$Horizontal\ Distance = \sqrt{Slant^2 - (3.6068\ m)^2}$$

As seen in Fig.6 the error between the true and average calculated horizontal distance for Trials 1-4 are 3.3746 m, 3.2949 m, 3.1390 m, and 2.7657 m, and has an uncertainty of 0.0905 m, 0.0243 m, 0.0156 m, and 0.0000 m, respectively. This data implies that the USBL precision is within the 5 meters that the Humminbird can provide with 95% confidence and is a valid substitute for a proof of concept.

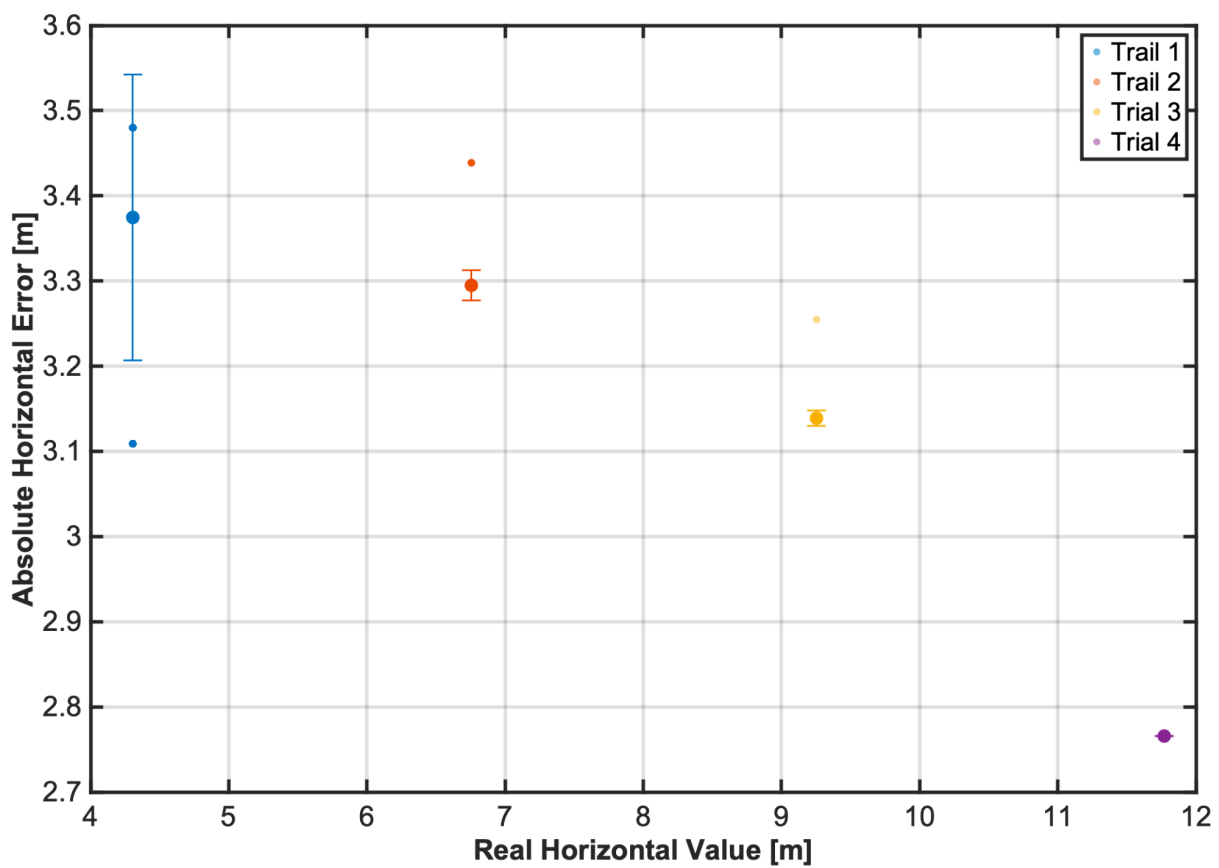


Fig. 7. Horizontal distance error vs true horizontal distance graph. The horizontal error across the distances measured is between three to four meters. This is only a one to two meter difference from UDel's five meter GPS error. The errors are similar enough to use the USBL system as a replacement for UDel's software during our tests.

Shown in Fig. 7, on average, the errors between the true slant distance and the measured slant distance for the four trials are 2.1227 m, 2.8333 m, 2.9671m, and 2.7193 m, respectively. The error uncertainty for these trials is 0.0905 m, 0.0243 m, 0.0156 m, and 0.0000 m, respectively. This data suggests that using the USBL system alone, we can track our ROV within three meters of its true position. This means that in the real-world worst-case scenario, with the USBL system and UDel's coordinates, we can guide the ROV within eight meters of the true location of a lobster pot before we need to switch to the onboard sonar and camera. However, for our testing, since we are utilizing a second USBL transceiver to determine the GPS of the lobster pot, the maximum error from the true pot location would only be six meters. If integrated with the DVL, the position tracking error will improve significantly. This will be discussed more in the controls section.

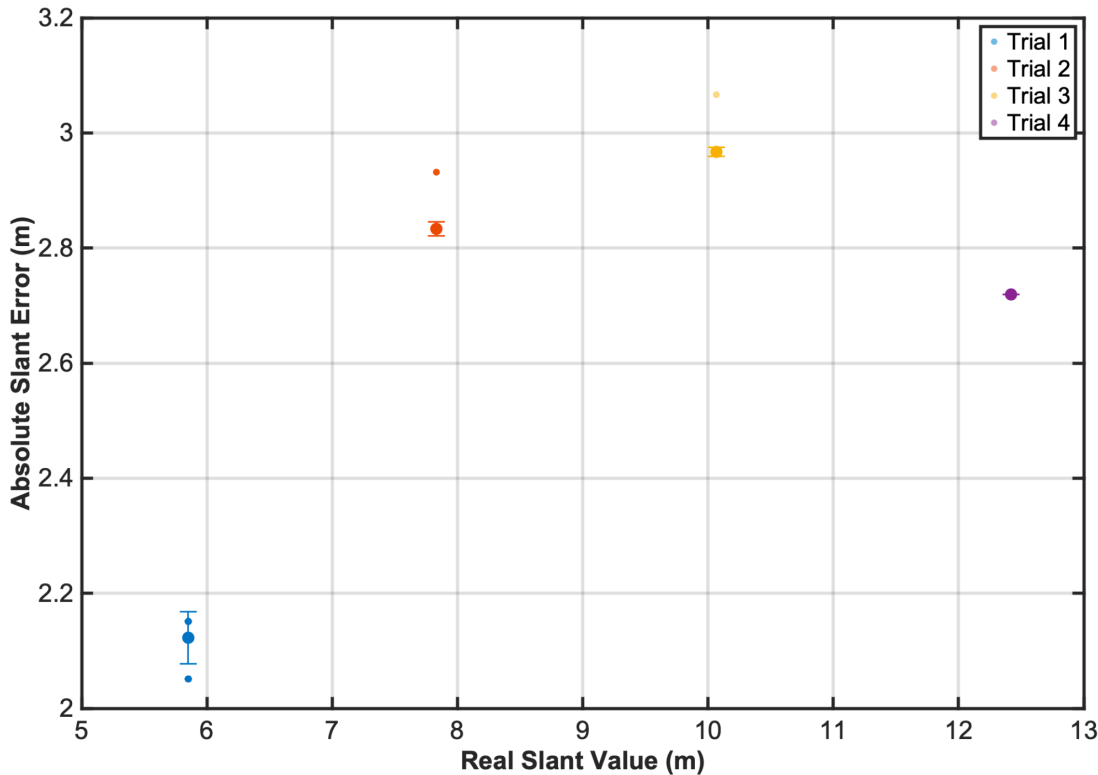


Fig. 8. Slant distance error vs true slant distance graph. The slant distance error across the distances measured is roughly two to three meters. From this data, we can assume that the true ROV position is within three meters of the GPS position given by the USBL.

Looking at the bearing error vs slant distance graph, shown in Fig. 8, we can see that

Trial 1 has a large difference between the true and measured bearing. In contrast, Trials 2-4 all fall within 20 degrees of the true bearing with 95% confidence. Further data will need to be collected to identify a relationship between bearing error and slant distance, however, we see the bearing error is most concerning at short distances. As we plan to switch to sonar and camera navigation at short distances (between six to eight meters), we believe that this bearing error will not affect our ability to successfully locate the lobster pot.

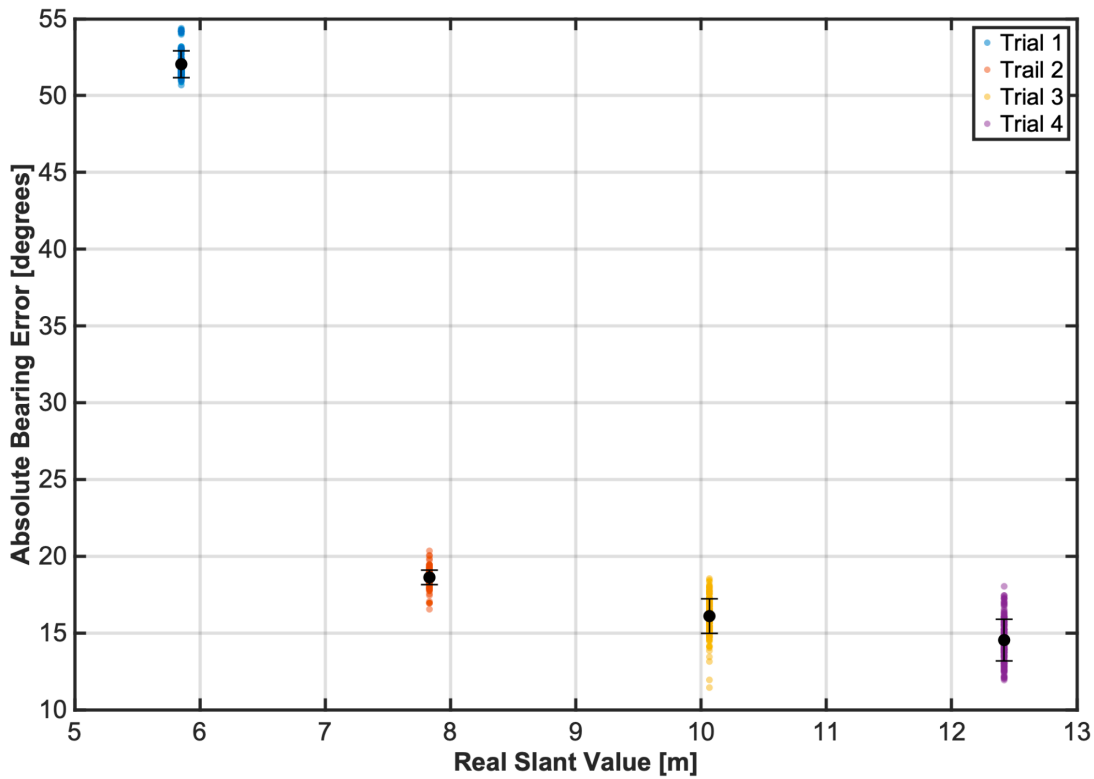


Fig. 9. Bearing error vs true slant distance. The bearing error spikes when the true slant distance is small (roughly 5.85 meters). At this distance, the ROV system will switch from USBL navigation to manual navigation using the ROV sonar and camera. Thus, short-distance bearing error poses no issue.

Once our system has determined that our ROV is at the lobster pot's GPS coordinate, we switch to manual control and navigate using the ROV's onboard sonar and camera. These close-range sensors are necessary to locate the exact location of the pot, as our USBL-derived GPS coordinates are meant to only guide the ROV to the general location of the lobster pot. We have engaged in small-scale testing of manual pot retrieval at this distance and found these sensors to be sufficient to locate a lobster pot with a manual operator. Additionally, the camera is necessary to aim and pierce the lobster pot with the spear attachment.

To confirm that the ROV operator would be able to distinguish a lobster pot from the ROV sonar and camera, the ROV system was tested in the Charles River. We placed the lobster pot a predetermined horizontal distance from the ROV and characterized how easily recognizable the lobster pot was on the ROV sonar and camera. Fig.10 shows that at roughly seven meters away, within the maximum positioning error range, the lobster pot is easily distinguishable on the sonar screen. The pot signal on the sonar is of higher intensity than the surrounding signals, and the box outline is clearly identifiable. The ROV operator will likely have very little difficulty identifying the lobster pot using the ROV sonar in real-world conditions.

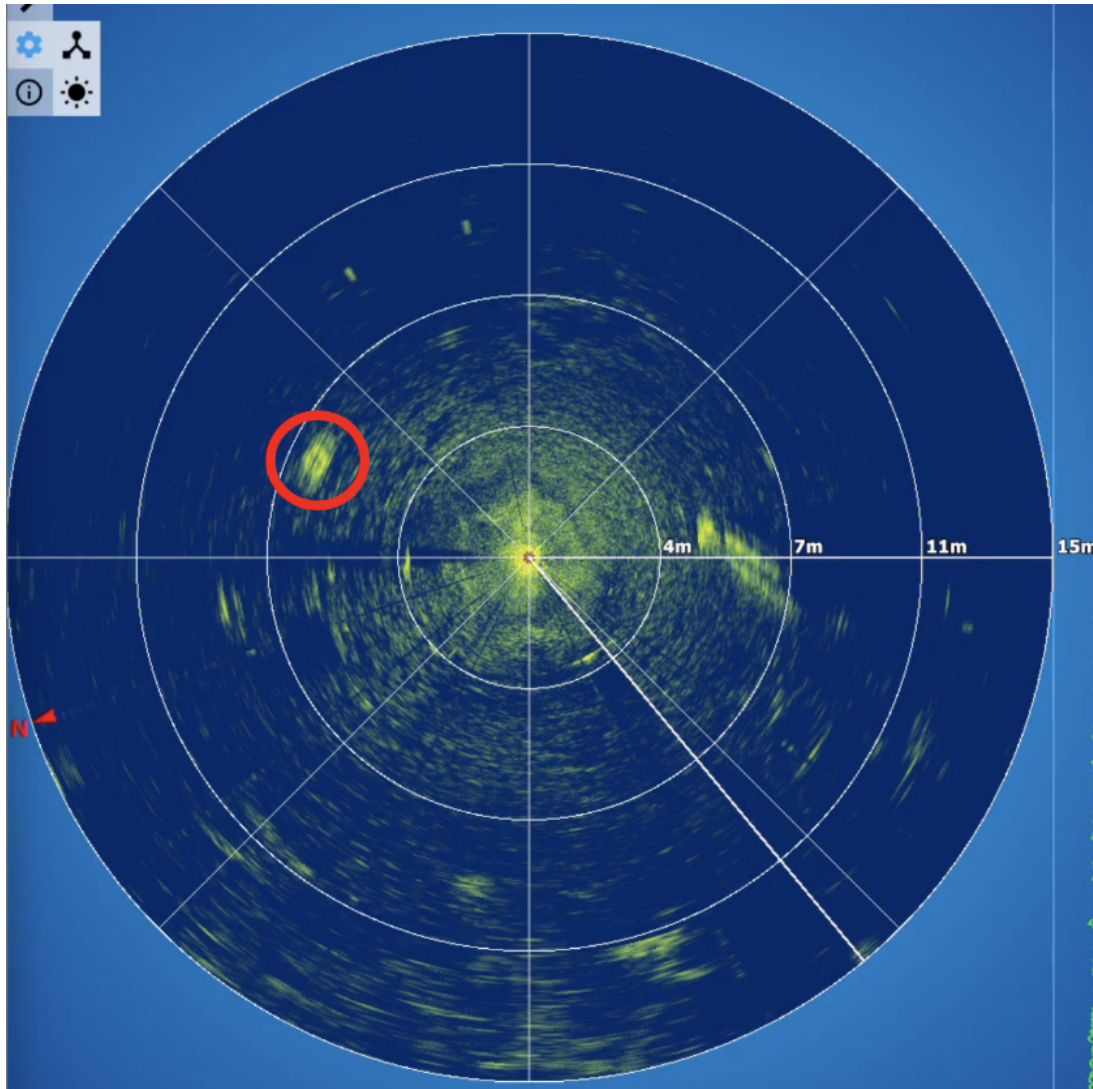


Fig. 10. Output screen of the ROV sonar with the lobster pot circled in red. With the sonar range set to 15 meters, almost twice our expected maximum error, the lobster pot is still clearly visible on the sonar screen. The ROV operator will likely have very little difficulty identifying the lobster pot using the ROV sonar in real-world conditions.

During the Charles River testing we were unable to visually identify the lobster pot using the camera until the ROV was roughly one meter away from the pot (Fig. 11). Thankfully, the pot is easily detectable on the sonar screen and thus the lack of visual clarity from the camera is not an issue. The ROV operator can rely on the sonar in turbid waters and simply use the camera

to aim. Additionally, the Charles River is equally or more turbid than lobster fishing areas, and thus we expect the camera range to be the same or better in actual lobster retrieval conditions.

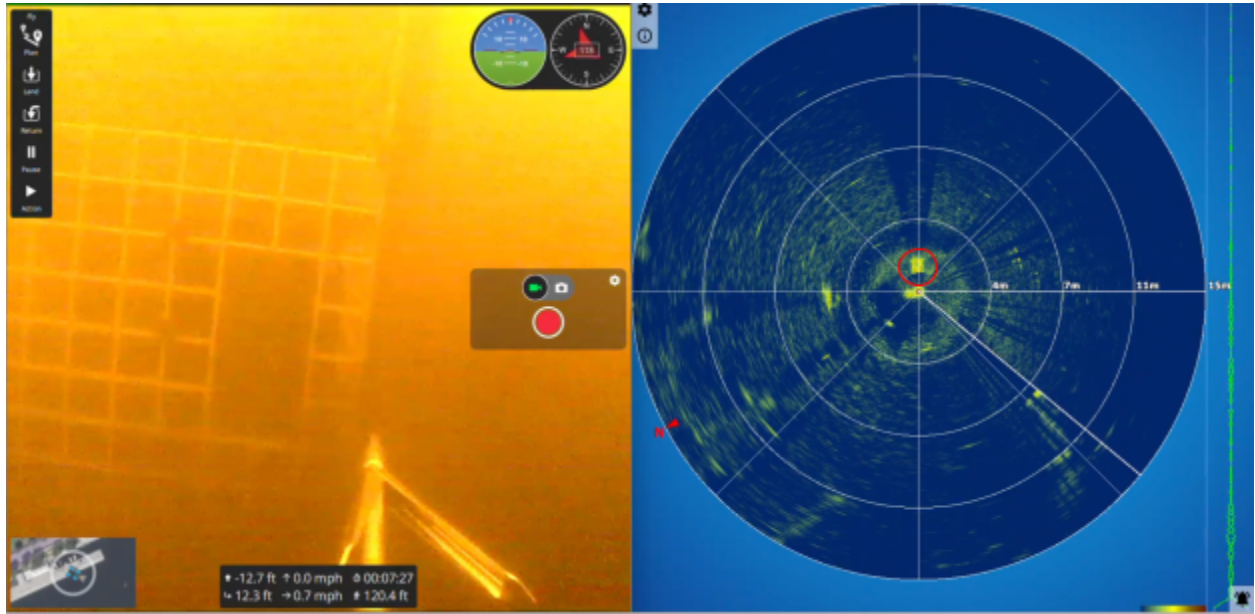


Fig. 11. Left: View from the ROV camera when the lobster pot was roughly one meter away. Despite the turbidity, the grids of the pot were clearly visible. Right: view from the ROV-mounted Ping 360 when the pot was roughly one meter away. Note the pot is still very clear on the sonar screen at this distance meaning that the ROV operator can rely on the sonar in turbid waters and simply use the camera to aim.

B. Potential Failure Modes

Robust localization requires predicting failure modes and taking steps to avoid them. Each component of the localization stack has its own vulnerabilities to consider during system design and mission planning. Components such as the DVL, USBL, compass, and sonar are essential for mission success and are therefore of particular interest. The DVL has two major failure modes. First, the DVL must remain within range of the sea floor to return useful velocity data. Second, low reflectivity floor surfaces can cause failure by scattering or absorbing the DVL signal. Multipathing can also cause DVL failure, but this should be less common in real-world conditions. The USBL has three major failure modes. The effective range of the USBL is

limited, especially at high frequencies. Given this, there is a maximum effective depth for accurately localizing the ROV in real-world conditions. USBL accuracy degrades over time due to drift and synchronization issues. Signal attenuation becomes a concern in occluded or turbid environments, such as those with significant silt or structural clutter, where acoustic signals may be scattered or absorbed before reaching their target. Similar to the DVL, multipathing can cause failure, but it should be a lesser concern in real-world conditions. The onboard compass provides an additional failure point. Significant heading errors can arise from localized magnetic interference, especially from nearby ferromagnetic deposits. This failure mode is typically detected during the pre-flight check when calibrating and is therefore avoidable. Sonar-based localization can be distorted if the ROV experiences motion during a scan. This is a greater concern in high-current environments where the ROV cannot hold position during a scan. In the case of total localization failure, we intend a two-step approach. First, attempt to have the manual operator localize. If this is not possible, then we move to having the ROV resurface. At the surface, we attempt relocalization, then ROV retrieval if localization fails.

IV. Navigation

The navigation system needs to command autonomous driving of the ROV by utilizing the coordinates retrieved by the localization team. We explored two methods of autonomous commands: 1) a custom PID controller for navigation via a Python script and 2) utilizing QGroundControl to control the ROV and send it given waypoints. We decided to explore the second method because it proved more applicable to our real-world system.

Initially, we developed a program that would work in parallel with the localization team's program that pulled in GPS data from the USBLs on the ROV and lobster pot. Using those

coordinates, our program would change the heading of the ROV to face the lobster pot while moving with a constant forward and downward velocity as it moves in the direction of the lobster pot. Over the course of a loop iteration, the latitudes and longitudes from the USBLs would recalculate the heading setpoint to ensure accuracy as the ROV gets closer to the pot. Our PID controller would manage the heading and depth of the ROV.

During this process, we discovered we could use QGroundControl and ArduPilot to control the ROV with waypoint navigation through the USBL and DVL, which can provide an accurate position of the ROV in the world. Using this system, we could still enter the provided coordinates of the lobster pot on QGroundControl to autonomously drive the ROV to the pot. QGroundControl also offers other useful control modes, including depth hold, position hold, and manual driving that may be useful if the operator needs to interrupt autonomous navigation. Since ArduPilot has multiple controllers built in for rate, velocity/position, roll, and pitch alongside heading and depth, the driving is significantly more stable than what would be achievable by our custom PID controller.

A. Communication Protocol

The ROV is equipped with a Raspberry Pi and a navigation board, which work together to handle communication and control. The Raspberry Pi runs BlueOS, which manages key onboard systems such as control logic, camera streaming, and tethered communication. BlueOS communicates over Ethernet via the navigation board and is capable of sending and receiving MAVLink messages through a designated UDP port. Both QGroundControl and our custom PID controller interface with the ROV by sending commands to this UDP port. When the USBL transmits GPS data to the receiver, QGroundControl receives it in NMEA format, parses it, and converts it into MAVLink messages to be forwarded to the ROV.

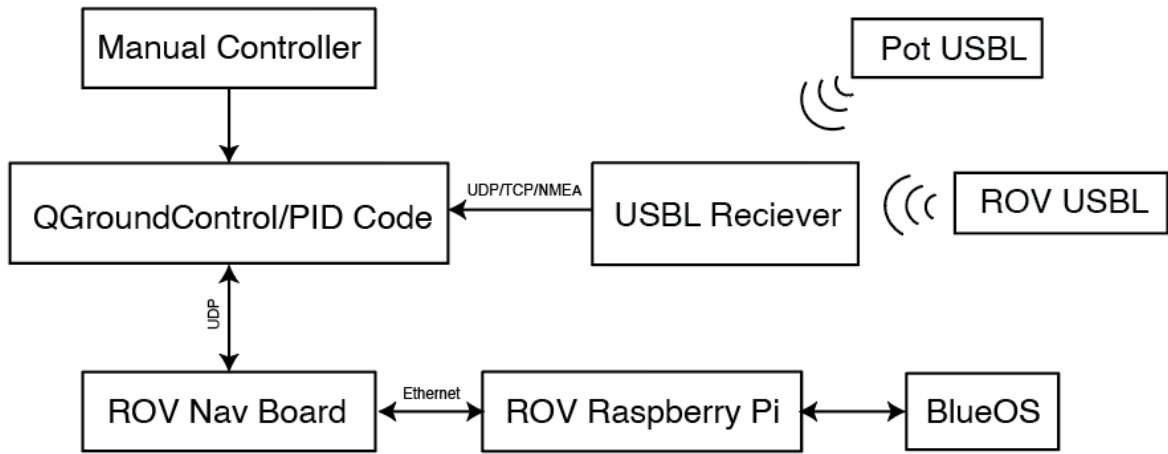


Fig. 12. The communication protocol for the navigation of the ROV.

B. Driving Process

Preparing the ROV and driving it to waypoints involves coordinating several software tools, including QGroundControl, Cerulean Tracker, and the BlueOS web interface. QGroundControl is used to send navigation commands and manage autonomous waypoint missions. Cerulean Tracker and BlueOS, on the other hand, are primarily used for system diagnostics and verification. Cerulean Tracker allows the user to confirm that the USBL receiver is functioning properly and that both the USBL and topside GPS are providing valid positional data. The BlueOS interface is particularly useful for monitoring the ROV's onboard systems, especially the DVL, to ensure it is outputting sensible data and that there is not too much accumulated uncertainty.

The preflight check for the ROV begins with verifying internal pressure and connecting the tether to the control computer. Once connected, the operator should power on the ROV and listen for the USBL to begin clicking, indicating it is active. While waiting, the operator should then manually test each thruster to confirm that all of them can turn on and drive in the right direction. The ROV is then ready to be placed into the water. In parallel, the operator should also

connect the USBL receiver to the laptop and wait for it to complete time synchronization on Cerulean Tracker before submerging the receiver. It is important to carry out the preflight check efficiently, as the ROV should not remain powered on outside of the water for extended periods to avoid overheating the DVL.

After the ROV is placed in the water, the GPS data is verified using Cerulean Tracker. The system must report a valid slant range to the ROV, and the topside GPS should remain a consistent minimal coordinate. Next, the BlueOS interface is used to inspect the DVL. On the DVL configuration page, the vehicle's starting position is set to match the current topside GPS coordinates, followed by calibration of the DVL's internal gyro. Once these steps are complete, the velocity and position outputs are monitored to ensure reasonable values, and the reported uncertainty is checked to confirm it remains below approximately three meters, indicating reliable DVL performance.

C. Testing

We had several rounds of testing at the Sea Grant small tank, in the Zesiger Center diving pool, and in the Charles River at the MIT Sailing Pavilion. Sea Grant was the place of initial testing for our concepts and major debugging. In both Sea Grant and the pool, one issue was the lack of reliable topside GPS, which made it difficult to use the USBLs effectively for position hold and waypoint navigation. To work around this, we implemented a Python script that simulated a GPS input by sending a fixed position to the system, allowing us to test controls in both the pool and Sea Grant. The DVL uses the Doppler shift of the four beams to calculate motion. The beams are intended to hit the bottom at an angle, which doesn't work on the smooth tank bottom. We attempted to mitigate this by placing carpets and towels on the floor to diffuse the acoustic reflections and provide a better reflective surface, which proved effective. However,

testing in the Sea Grant test tank remained challenging due to the DVL's margin of error, which typically ranges from one to three meters. While this level of uncertainty is acceptable in open-water environments, it becomes significant in the constrained space of the tank, where small errors can lead to large deviations relative to the environment size.

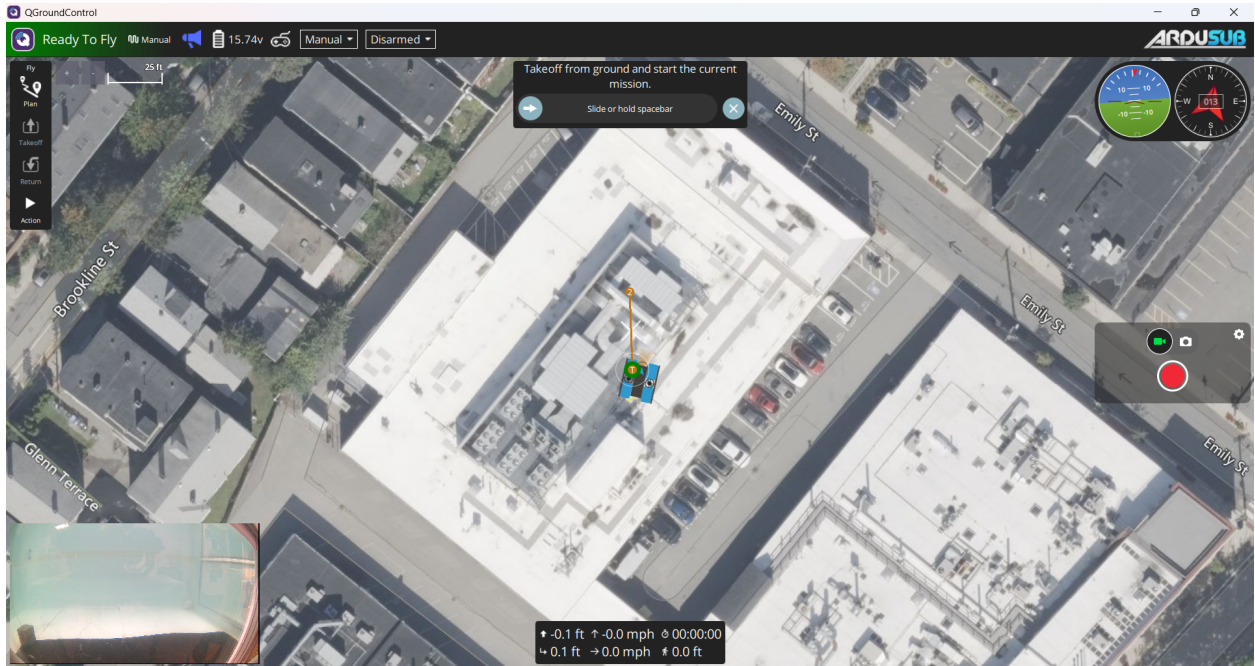


Fig. 13. Screenshot of QGroundControl waypoint testing at Sea Grant.

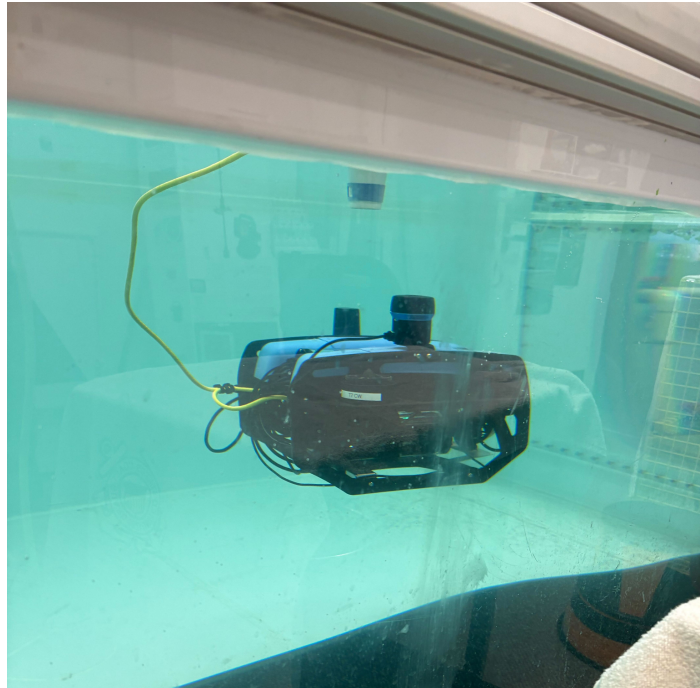


Fig. 14. Our ROV holding position in the Sea Grant tiny tank using USBL and DVL.

D. Issues and Debugging

We encountered several recurring issues during testing that impacted the ROV's performance. First, the DVL is highly sensitive and prone to overheating when operated outside of water, which makes it essential to complete the preflight check quickly. It takes about 20 to 40 minutes for the DVL to overheat. Another common issue was discrepancies between the GPS data shown in Cerulean Tracker and what appeared in QGroundControl; we used QGroundControl's Analyze Tools to inspect the MAVLink messages being received by the ROV, though the root cause of the mismatch is still under investigation. Finally, we often faced errors when switching into AUTO mode to begin waypoint navigation—this was typically caused by the DVL not receiving a valid vehicle position from BlueOS, due to an incorrect or unset system parameter. Below is a table of all the parameters that are good to check when debugging.

Table 1. The BlueOS parameter settings for the ROV system.

Parameter	Setting
AHRS_EFK_TYPE	EKF3
EK3_ENABLE	Enabled
VISO_TYPE	MAVlink
RNGFND1_TYPE	MAVlink
EK3_SRC1_POSXY	GPS
EK3_SRC1_VELXY	External Nav
EK3_SRC1_POSZ	Baro
GPS_TYPE	MAV

The ROV we worked with was relatively old, so the sensors required frequent calibration and still encountered functionality issues. The electronics inside the ROV were tightly packed, which often led to shorts that needed troubleshooting. While these issues could be time-consuming to resolve, they provided valuable insights into how the ROV operated and the limitations of the sensors.

E. Navigation Conclusions

We have established the foundation for autonomous navigation, but due to limitations in our testing locations and time constraints, we were unable to complete the full implementation. The DVL adds an additional layer of complexity, and its necessity depends on the environment.

In clear water, waypoint navigation can be effectively managed using only USBL data. However, in murkier water, USBL data may lose accuracy, making the DVL essential. Regardless of whether the DVL is used, it is crucial that the navigation system is designed and tested in the actual deployment environment. This ensures that QGroundControl's PID parameters are accurately tuned within a margin of error needed given the environment.

V. Recovery

A. Overall Design Requirements

Intuitively, the success criteria of any novel method of ghost lobster pot retrieval should be assessed relative to the ease and speed of the existing method: hauling the pot in by hooking the pot's buoy-line up to a hydraulic winch. In the interest of limiting unnecessary changes to a verified process, we chose to take all aspects of the lobster boat and winch as given. Our method, then, largely interfaces between two sets of constraints—those imposed by the lobsterman and his/her vessel at the surface and the BlueROV and lobster pot on the ocean floor.

1. Surface Constraints:

Our decision to utilize the lobstering winch imposed an upper loading constraint of 900 N on our system. The lobsterman's budget imposes an additional fiscal constraint. Finally, the chaotic movements of an ROV suspended from a winch on board a boat rolling and pitching at sea raise some safety concerns for designs with sharp objects.

2. Subsurface Constraints:

The compact BlueROV frame allows little space for mounting additional electronics enclosures. As a result, it was desired that our method make minimal additions to the already overstuffed electronics enclosure. The standard lobster pot design imposes constraints of its own. The use of rope hinges for connecting pot lids to the rest of the pot makes the lid an unideal attachment point. There is, however, a strong central column at the top of the pot that serves as a more than adequate attachment point.

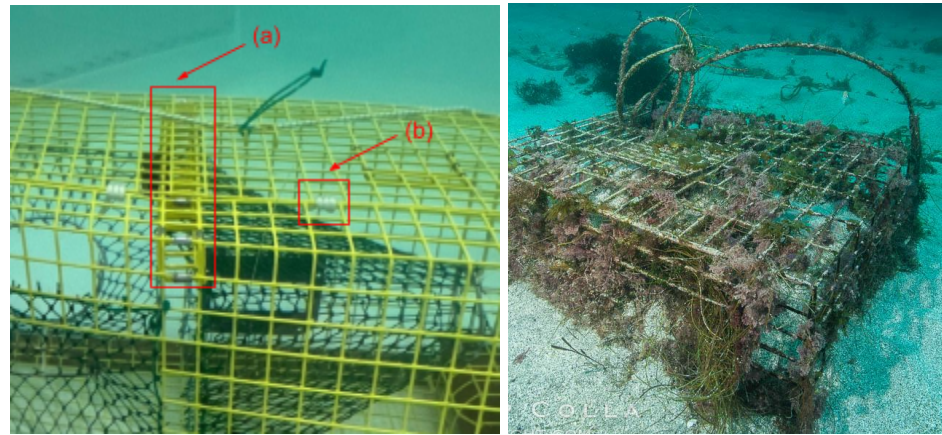


Fig. 15. Left: Lobster pot in MIT Sea Grant testing tank. (a) strong central column (b) rope hinges. Right: Stubbornly grounded ghost pot [4]. Note difference in grid geometry between the two pots.

It therefore seems desirable to have a system capable of targeting this central column in the event of the sides being blocked by debris or biofouling. Additionally, different pot manufacturers make pots with different grid spacing, so any retrieval method must be easily adaptable to variations in grid geometry. Finally, it's possible that some pots are so heavily grounded that the required lifting force exceeds the 900 N lifting capacity of the winch. In this case, some sort of breakaway mechanism to free the boat from the stuck pot is imperative.

These constraints produced the following design requirements for the retrieval method (in no particular order): (1) loading requirement: the method must be able to tolerate $\geq 900 \text{ N}$ (2)

safety requirement: the method must be safe to use on the deck of a rolling lobster boat (3)
ergonomic requirement: this requirement takes into account the cost, in time and money, to the
lobsterman—including manufacturing costs associated with making changes to the ROV frame
(4) approach requirement: a reasonably skilled user should be able to choose their attachment
point (5) adaptability requirement: the method must be adaptable to grids of various size (6)
disengagement requirement: the method should include some means of detaching from pots that
prove too stubbornly grounded for the winch to lift.

B. Tethered Connection

The basic BlueROV tether, rated to ~1300 N of tension, more than satisfies the loading requirement. The interface between the tether and the ROV's electronics housing, however, is not rated. Blue Robotics sells a nylon thimble that, when zip-tied to the ROV frame, acts as a strain relief (Fig. 16).



Fig. 16. Picture of the nylon thimble Blue Robotics sells for use as a strain relief.

A back-of-the-envelope analysis of the BlueROV frame, modeling the attachment point as a beam rigidly fixed at both ends subject to point loading, showed it was more than capable of handling these loads. Further analysis with Fusion360's FEA tool concurred.

However, though sufficiently strong, this sort of static strain-relief forces the tether to pull out of line with the hook, creating undesired moments as the ROV is retrieved. Additionally, the current attachment method uses zip ties that could potentially cut into the cable when tension is applied. To overcome this, we recommend stringing a braided rope across the back of the ROV frame as a tether attachment point, then threading the nylon thimble onto the braided rope. This ensures the tether always pulls along the same axis as the hook and distributes the load across the entire ROV frame instead of a single side. While we **did not** implement this set-up for the demo—due to limited time and the minimal loads on the ROV during the demo—we are fairly confident of its efficacy based on reports by other members of the Blue Robotics community who use a similar set-up.

C. Engagement

We considered several engagement mechanisms defined by various characteristics, including static vs actuated, number of points of contact, and types and methods of contact.

Static Hook

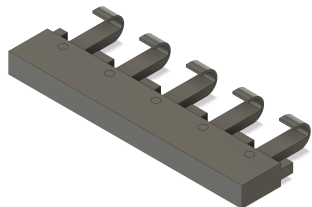


Fig. 17. Static hook array.

This design features a standard, static, hook—either in an array or as an individual. We planned to plant a shear-pin between the hook/hook array and the ROV frame to ensure disengagement at loads >900 N. This is the most straightforward design with the least amount of failure points and mechanical complexity, making this a safe option with a higher chance of success relative to the time and materials required for the design. Fig. 17 depicts a 1-dimensional array of static hooks attached to a pivot point, which allows for some tolerance as the ROV engages with the grid of the lobster pot. It uses a one-prong hook design to allow for a disengagement sequence by simply moving the ROV correctly. However, the array's primary advantage can also be disadvantageous if the alignment between the ROV and the ghost pot is poor or if only a fraction of the hooks make a successful engagement.

Spear Hook

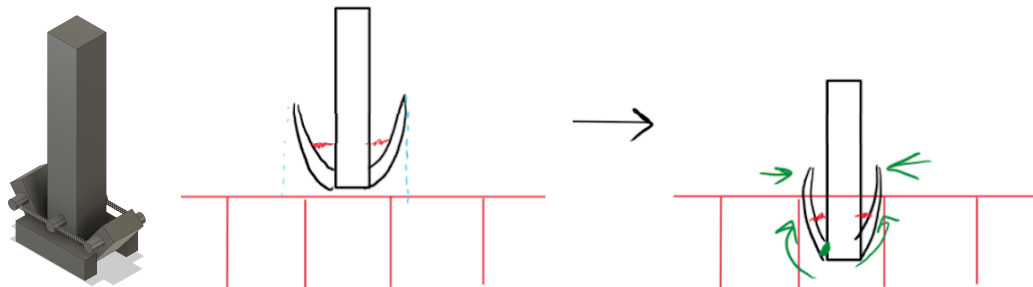


Fig. 18. Left: CAD model of the sprung spear hook. Middle: Spear hook in its unengaged configuration. Right: Spear hook in its engaged configuration.

This design uses a barb modeled after those used in spear fishing with a passive engagement and disengagement mechanism. When the barb goes through one of the ghost pot's grids, the barb folds together to allow for entry and unfolds once fully inside, preventing the lobster pot from disengaging. In the case of a heavily grounded pot, the springs are sized such that the maximum torque applied by a 900 N pot on the springs exceeds the springs' max torque--allowing the barbs to fold down and slip out of the pot.

Actuated Hook

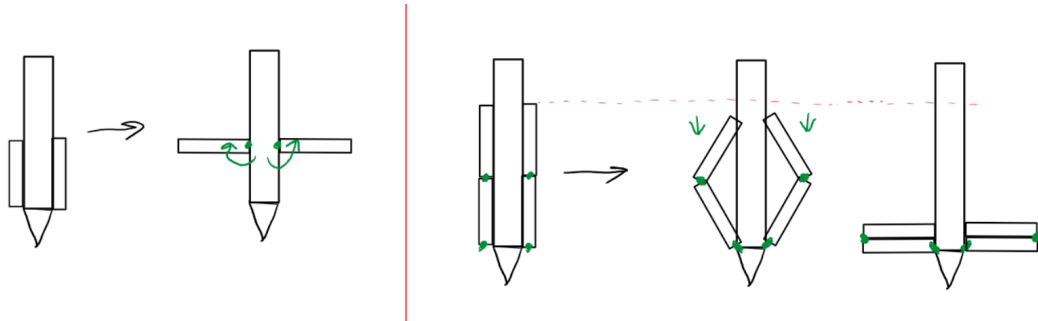


Fig. 19. Left: Sketch of the flap-based version of the actuated hook. Right: Sketch of the car-jack version of the actuated hook design.

This actuated hook design would have used waterproof actuators to engage and disengage the pot. The design on the left shows two flaps that can fold out to come into contact with the grid while the design on the right depicts a linkage mechanism similar to a car jack. Both designs can use either a linear actuator to drive the motion so that the extension positions can be held at high forces without being driven, or they can be directly driven by motors. Active engagement and disengagement remove the potential of the ROV getting stuck and needing to break off the hook since the position and engagement of the ROV can be adjusted at any time; however, this comes at the cost of a heavy electronics modification to the ROV, additional weight, increased complexity and development time, and points of potential mechanical failure.

Compliant Hook



Fig. 20. Sketch of proposed compliant hook design.

Considered both as an array and an individual hook, this design features hooks connected to the ROV by a flexible joint, allowing nearly unrestricted motion in all 6 degrees of freedom. A shear-pin interposed between the hook and the ROV fulfilled the breakaway requirement.

Soft Robotics:



Fig. 21. Depiction of filament-like soft robotic actuator developed by Prof. Kaitlyn Becker [11].

This design, modeled after the filament-like actuator developed by Prof. Kaitlyn Becker, would have used soft, likely silicone based, tentacles to actively entangle the lobster pot before contracting under hydraulic actuation. While such a design makes engaging the pot with the ROV almost trivial and distributes load across the surface of the pot, the complexity of actuating

such a mechanism, and the quantity of uncertainties in the manufacturing process, ultimately sank this design.

The Hugger

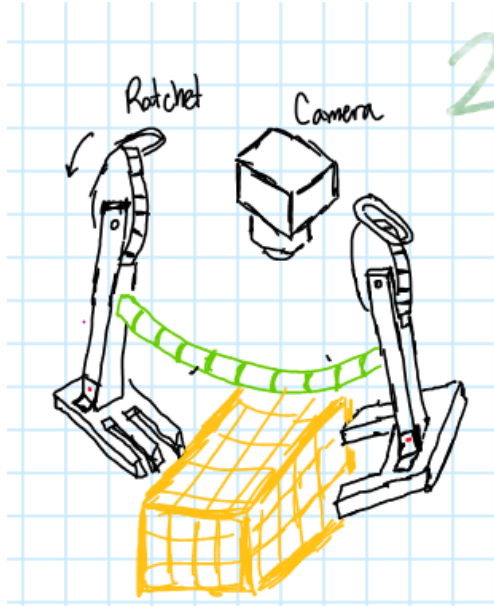


Fig. 22. Sketch of the hugger mechanism.

A sort of one-way latch, the Hugger uses gravity to lock the arms into the grid of the pot. Each arm is mounted to a gear with a ratchet that prevents the arms from opening during the lift process. Since the arms are gravity-actuated, the distance between their pivots would have to be manually adjusted to the desired pot size before deployment. Manufacturing complexity was also a concern.

Design Choice

We used a Pugh chart to evaluate each design's ease of use, ease of manufacture, clamping strength, chance of disengagement, ease of disentanglement at the surface, possible danger to the operator, cost, and overall robustness to failure.

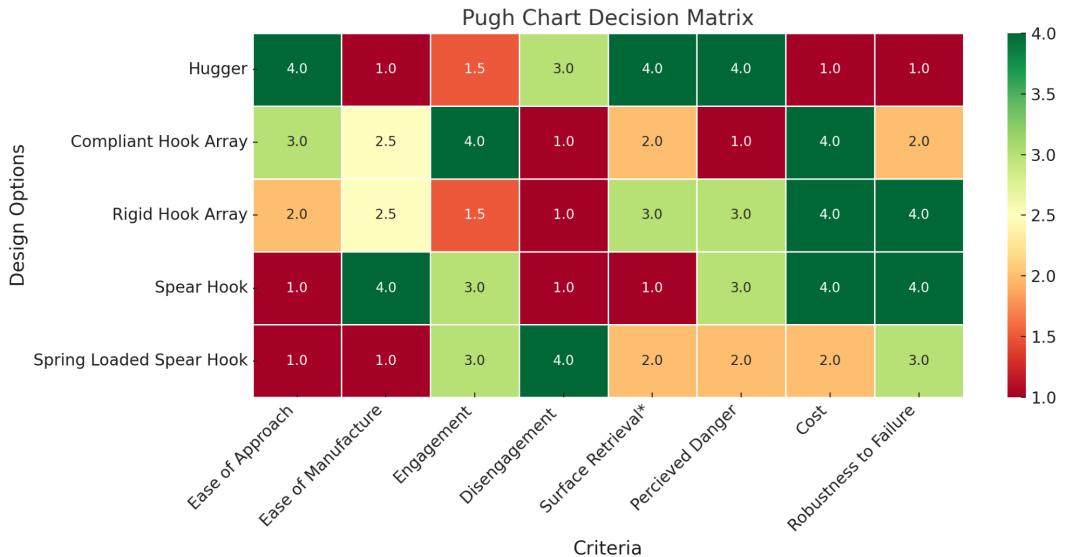


Fig. 23. Pugh chart used to assess each design. We eventually decided to go with a (modified) version of the spear hook.

The results pointed towards using the sprung spear hook sans spring since we could not find a spring with the necessary strength that was also a workable size. Instead, we decided to use a shear-pin to fulfill the disengagement requirement.

D. Initial Prototype

Prior to the first pool test, we assembled a simplified version of the final spear mechanism. This initial prototype used an off the shelf 7 mm spear-fishing barb fastened to a 6 mm threaded stainless steel rod via a 2 mm screw/pin. This spear was then locked onto a C-channel—using nuts to book-end the front and back of the channel—which was mounted to the bottom of the ROV.

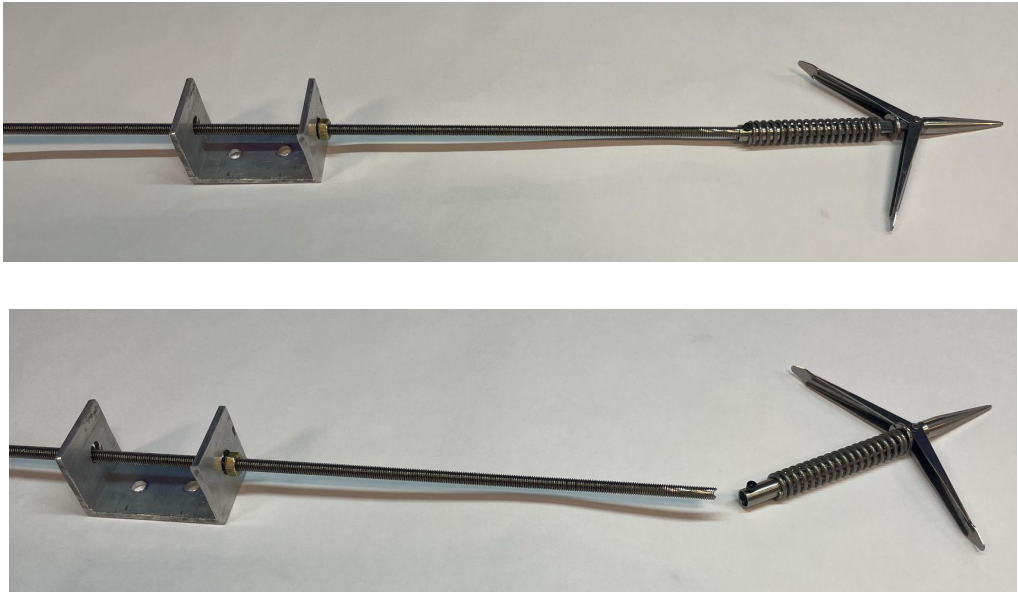


Fig. 24. Top: Picture of the prototype spear prior to the first pool test. Bottom: Picture of the prototype spear after the first pool test. The barb broke off when subject to unexpected moments while removing it from the pot.

During the test, the ROV was piloted to spear a pot dropped at the bottom of the pool before being hauled up by its tether. Once at the surface we attempted to dislodge the barb from the pot—and in the process snapped the 6 mm threaded rod. The entire process offered several key takeaways:

1. There must be an easy way to “disarm” the ROV—this limits risk to the user when the ROV is at the surface but not yet deployed.
2. The spear must minimize the number of things that need to be screwed on/off before deployment since residual water makes applying any sort of axial torque to the rod by hand nearly impossible.
3. A stronger rod was necessary.
4. There must be an easy—consistent—way to dislodge the barb from the pot. This improves retrieval efficiency, user experience, and exposes the spear assembly to less risk of failure due to frustrated manhandling.

As a result, we revisited our initial design concept. In light of the first two takeaways, we added a latch-box to the ROV. This allowed easy addition and removal of the spear from the ROV without the need to rotate any potentially wet parts. In answer to the third takeaway, we began a series of hand calculations and FEA simulations to appropriately size the spear shaft. Finally, in making these changes, we discovered we'd also addressed the fourth takeaway—the addition of a “latch box” made removing the spear from the lobster pot trivial—the user could simply drop the ROV end of the spear out of its latch-box-housing, replace it with a new, pot-unencumbered spear, and redeploy the ROV before returning to the task of removing the previous spear from the recently retrieved pot—a task made significantly easier by the lack of a 9 kg ROV at the hilt end. This workflow had the added benefit of introducing redundancy into the design. Since each spear is relatively inexpensive, ~\$50 at the most, a lobsterman can easily carry half a dozen with them on each mission. Then, in the event of a barb breakaway, the lobsterman simply needs to switch out the spear in the latch-box instead of going through the more intensive process of replacing the breakaway mechanism on the deck of a rolling boat.

E. Mechanical Fuse

Based on the unsprung spear hook design that is being used at the end of the spear assembly, a mechanical fuse is required for emergency disengagement with a stuck lobster pot. The two mechanisms we explored using for this feature were a snap shackle and a shear pin.

Snap Shackle



Fig. 25. CAD of the snap shackle design.

A snap shackle assembly would offer multiple desirable characteristics. The snap shackle itself would be purchased off the shelf from a manufacturer. This means the part does not need to be custom machined and will be well tested and rated to break under a specific load. Our assembly, as shown above, would have the snap-shackle connected to threaded rods on either end with a sheath covering the shackle and connection points.

This design does present some engineering challenges. First and foremost, in the event that the hook snaps off, this design would require that the sheath and the remaining half of the snap-shackle be removed before replacing the snap-shackle and barb. This would require multiple steps and likely some hand tools, which is less than ideal.

There is also the challenge of connecting the snap shackle to the threaded rods. We intentionally left this as a placeholder in our design because drilling a hole into the rods would either make them weaker than the snap-shackle or, if the holes were sufficiently small, the connecting component would be weaker than the snap shackle. One solution would be to connect the rods to more sturdy pieces and connect the snap shackle to the larger pieces, but this only adds cost, weight, bulky geometry, and complexity to the system.

Finally, using the eyes as connection points means that the barb side of the assembly will not be entirely constrained in pitch, roll, and yaw. Our sheath design constrains pitch and yaw to smaller angles, but could still make hook engagement difficult for the operator to control and/or create undesirable or unplanned load conditions due to the system not having fixed geometry.

Shear Pin

For those reasons, we decided to go with a shear pin as a mechanical fuse, which is a more elegant design overall, but requires more modeling and fine tuning to fail under the correct load.

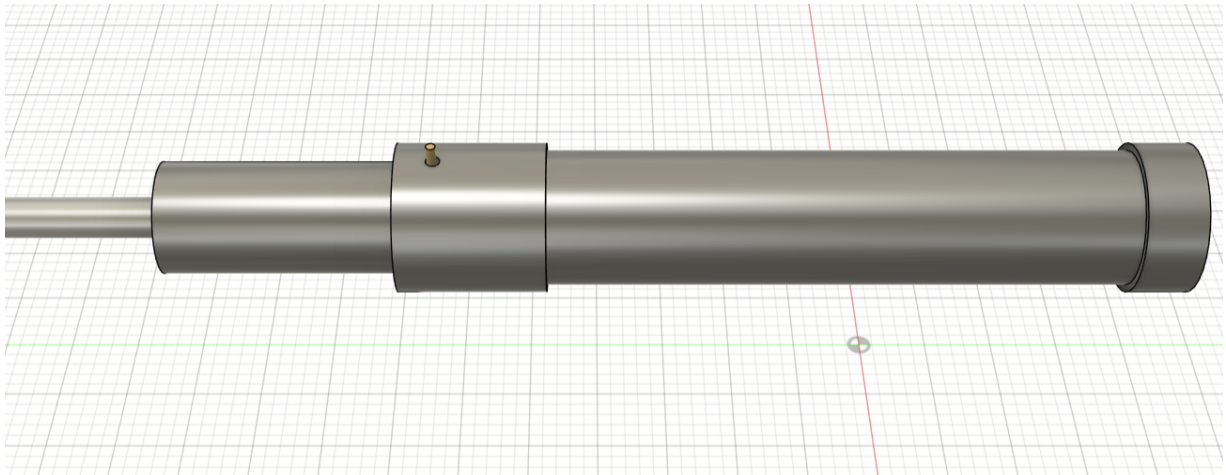


Fig. 26. CAD of the shear-pin design using a mortise-and-tenon joint.

Above is an image of the design for the spear assembly with the shear pin as a mechanical fuse. On the left side of the image is the threaded rod with the barb on the end of it. The threaded rod is screwed into a thicker metal cylinder that is part of a mortise and tenon joint. The joint is secured by a brass shear pin that acts as a mechanical fuse.

While the overall design is simpler than the snap shackle, we were forced to rely on our own calculations and experiments to verify the shear pin would break at less than the 900 N of tension. To accomplish this, we took four approaches: calculating the loads and resulting forces

by hand, using finite element analysis, conducting a gravity loading test, and conducting an Instron machine test.

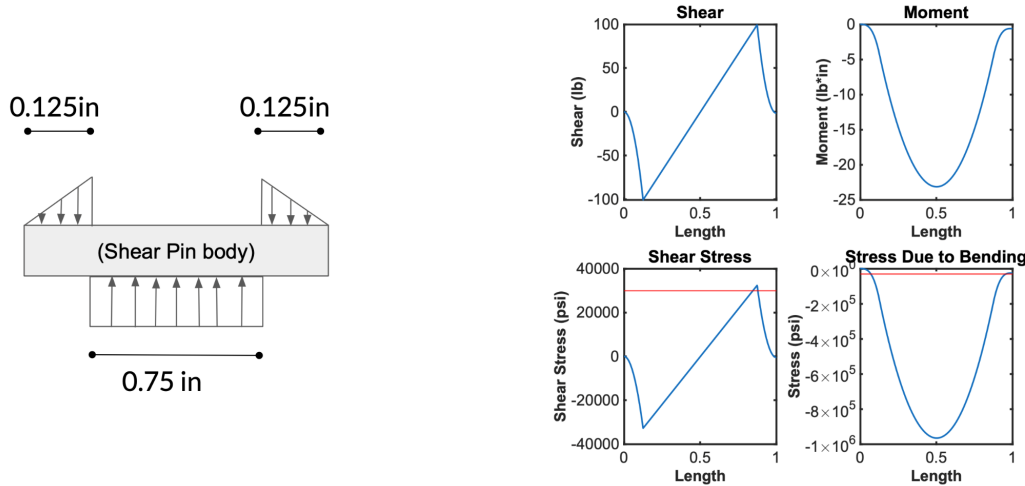


Fig. 27. Left: predicted loading model for shear-pin in a mortise-and-tenon assembly. Right: Matlab plots of shear stress and bending stress experienced by the pin under idealized loading conditions.

For the hand calculations, we treated the shear pin as a uniform cylinder undergoing perfectly radial loading. The diagram above shows how when the spear assembly is experiencing axial loading, the tenon joint will apply uniform radial load to the shear pin. To balance out both the forces and the bending moment at the boundaries, the mortise will apply triangular radial loading. The arrows in the diagram are purely for visualization and not drawn to scale.

Using this model, we were able to calculate the shear forces and bending moment experienced by the shear pin. Based on the assumed pin geometry with a diameter of 1/32", we calculated the shear stress and stress due to bending moment. All four of these are shown on the graphs in the image above, and the stresses shown in the bottom two graphs are plotted with a red line to represent the shear strength of the brass.

Based on the calculations above, it would appear that the 1/32" diameter pin would break just under 900 N due to shear stress, but would break considerably sooner in the event of

bending. Because we were unsure of which loading the model would be more accurate for, we utilized finite element analysis to model how the loading would affect the pin.

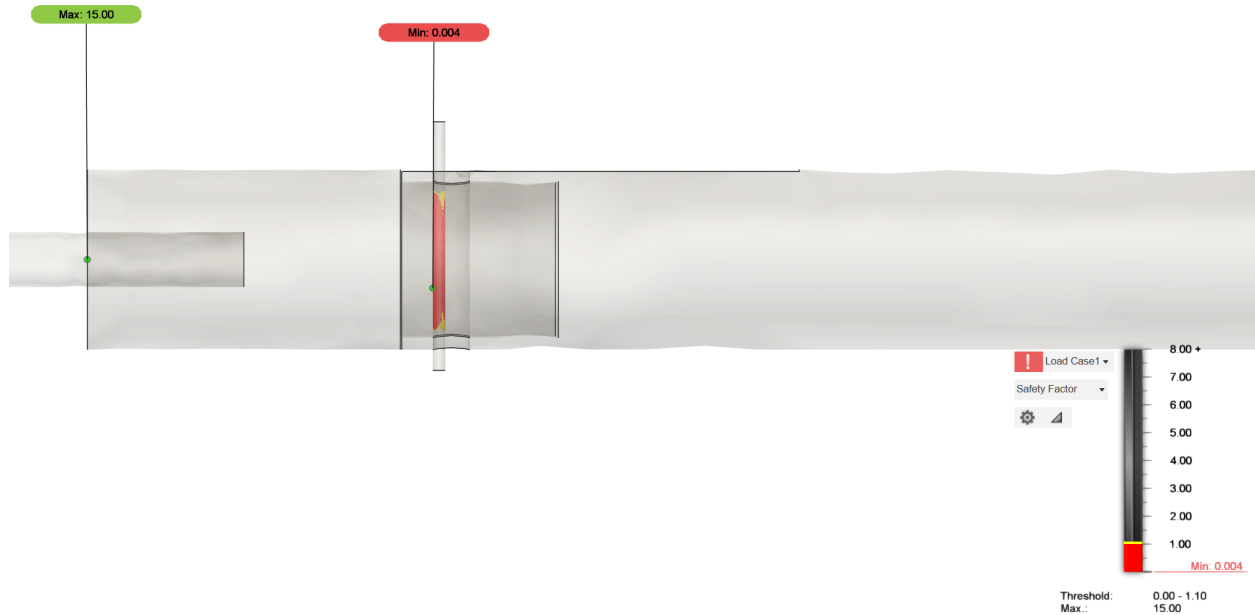


Fig. 28. FEA analysis of the shear-pin assembly in Fusion 360. Pin diameter is $1/16''$. Note that greyed-out sections have a safety factor greater than one.

The results of the finite element analysis indicate that a $1/16''$ diameter rod would fail 250 times over under the specified load conditions, however, this is not consistent with our hand-calculated model, which indicates that even if it fails due to bending moment, it should only fail four times over. We believe this discrepancy arises because Fusion's static-loading FEA tool is not intended to model parts past small deformations—much less total failure. At this point in time, the results were still considered inconclusive, so we designed two physical experiments in the hopes of finding agreeing results. The goal of these experiments was to test different shear pins ranging in size from the largest pin that would break under our model of bending moment stress ($3/16''$) to the largest pin that would break under our model of shear stress ($1/32''$).

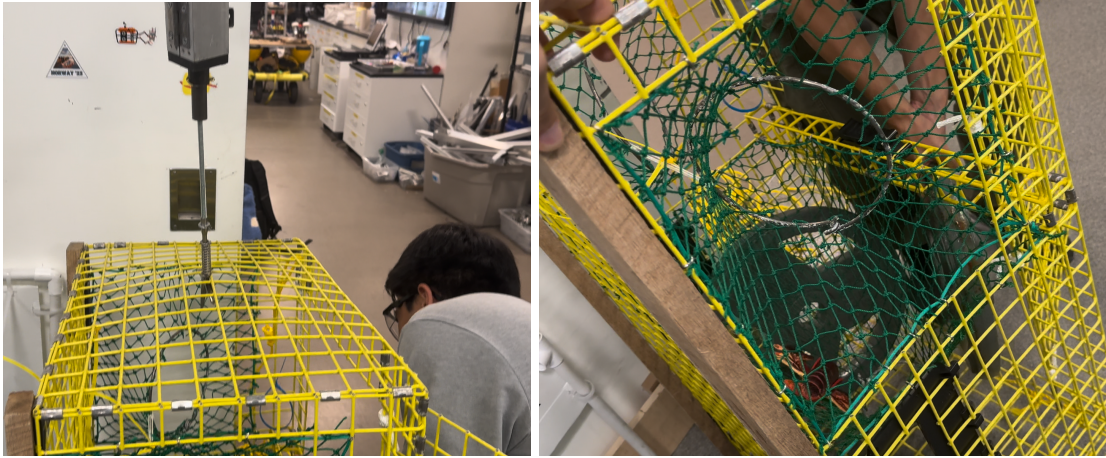


Fig. 29. Left: picture of the spear and latch-box assembly under tension. Right: picture of weights being loaded into the lobster pot. Note: smallest incremental weight was 22.2 N, so quasi-static assumption does not hold.

For the first physical experiment, we hung the spear assembly off of a pulley mechanism that could be used to raise and lower the spear. We engaged the spear with the top of a lobster pot that was resting on the ground and filled with weights to weigh 900 N. For each run of the test, we used shear pins of decreasing sizes and attempted to use the pulley to lift the lobster pot off of the ground. If the shear pin snapped without lifting the pot, its maximum load was presumed to be under 900 N, and it would move on to the next half of the experiment. The only pin that broke was the 1/32" pin.

The second half of the experiment involved finding the minimum load at which the pin would break. The closer this value was to 900 N, the better suited the pin would be for the system. This part of the test involved starting with the lobster pot hanging off of the spear empty without touching the floor. We added weights to the pot in increments of as small as 5 pounds until the pin broke. The highest weight the pin could support without breaking would be considered its rated break point. The results showed that the 1/32" pin could support up to 801 N on the end of the barb, a figure we were satisfied with but wanted to confirm with further testing.

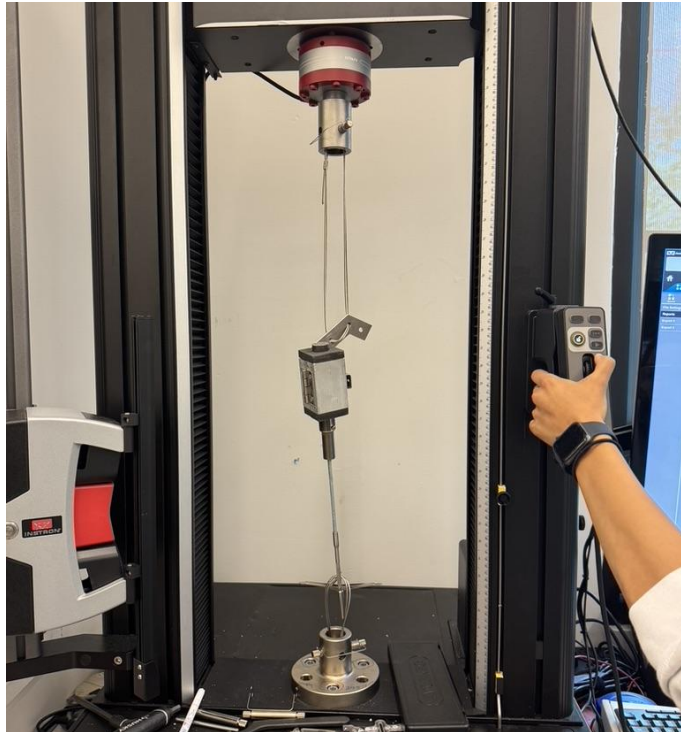


Fig. 30. Picture of the instron test. Machine applied constant strain at a rate of 20 mm/min.

The final test we conducted was an Instron pull test in which the assembly was subjected to constant axial elongation of 20 mm/min; Force and time data were recorded. The 1/32" pin was tested three times, and the results of the test are shown below:

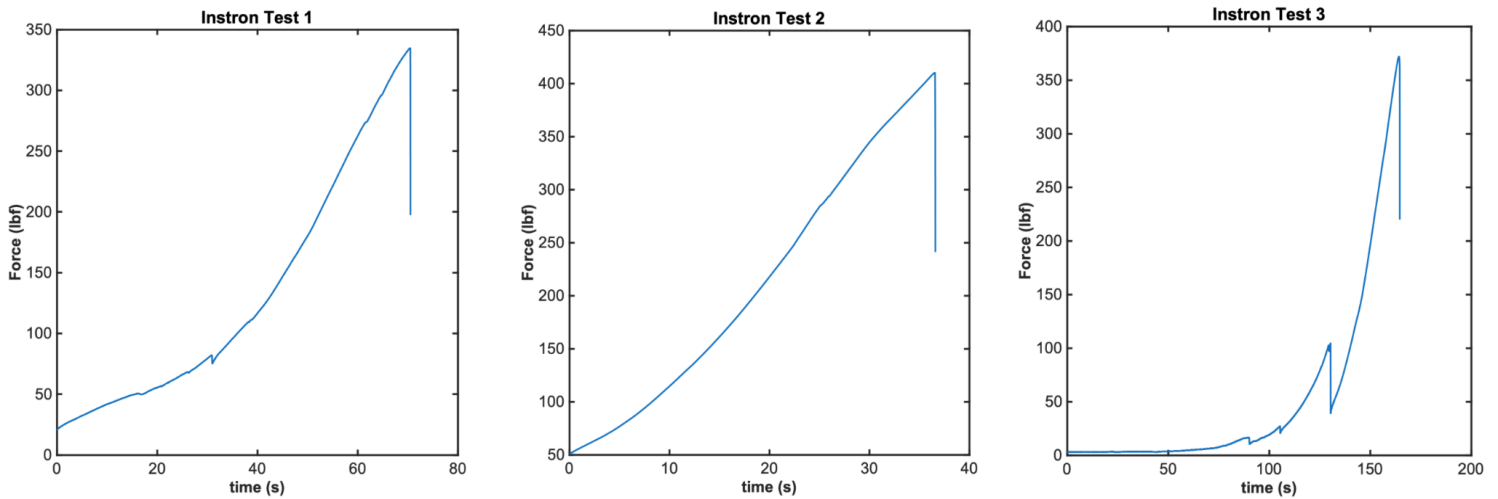


Fig. 31. Instron Test Graphs. We suspect that the downward spikes, most visible in Instron Test 3, was likely due to the tenon slipping inside the mortis.

In the first test, the latch came unclasped at 334 lbf (1486 N). In the second test, the pin snapped at 409 lbf (1819 N). In the third test, the pin snapped at 371 lbf (1650 N). While these results were unexpected and show that our shear pin does not yet achieve the initial desired effect, they do inform us about the mechanical capabilities and limitations of our system.

The tether our design uses to winch the ROV to the surface is rated to 1557 N. With slight improvement to our latching mechanism, we can ensure that our assembly will be stronger than the tether, meaning it will be sufficient for use in systems with stronger winches.

As for the discrepancy in experimental results, there are several factors that could be at play. Careful examination of the shear pin revealed that the cross section of the brass was not circular by the time the pin snapped (Fig. 32).



Fig. 32. Picture of cross section of 1/32" shear-pin. Note the non-circular cross-section.

This either means the pin started out with a non-circular cross section before starting the test, which would mean the initial calculations were incorrect, or it could mean that the pin flattened during the test. In the case of the latter, not only would the pin no longer behave the same way as it would in our hand-calculated model, but there may also be hardening effects that changed the mechanical properties of the pin during the test. Strain hardening could also have occurred as a result of the high tolerances in the pinhole geometry.



Fig. 33. Shear Pin assembly close-up. Note the large clearance of the shear-pin hole. We suspect this allowed significant deformation of the pin, resulting in different loading conditions than we initially predicted.

The pinhole was drilled based on the diameter of the largest shear pin we would be testing. This means that there was a lot of physical space for the 1/32" pin to bend and deform, which would have changed both the pin's mechanical properties—due to strain hardening—and resulted in significantly different loading conditions than those captured by our idealized

mathematical model. Both of these discrepancies could have contributed to the unexpected Instron results.

While the gravity test results seemed promising at first, the lower values may be a result of non-quasi-static loading or dynamic loads. In other words, if we raised the pot off the floor too quickly at the beginning of the test and lowered the weights into the pot too quickly at the end of the test, we would expect lower results than what we observed in the Instron experiment.

Ultimately, we do not have a shear pin that breaks at the desired load at this time, but we have promising results for future development. In all tests but one, the shear pin was the first part of the assembly to break, meaning it is the only part of the design that needs tuning to achieve the desired effect. Also, in the field, force will not be applied in a quasi-static way, and the gravity test is likely more accurate to how the assembly will respond to impulses in the real world.



Fig. 34. Left: Screenshot of full system CAD with the latch box closed. Middle: Screenshot of full system CAD with the top of the latch-box suppressed. Right: CAD of the full spear mechanism mounted to the ROV.

F. Spear System Summary

Based on our calculations, the shear pin was placed perpendicular through two collinear cylinders. The outer cylinder was placed inside a latch-box housing unit that opened across the middle with a hinge and latch mechanism to allow for the easy removal and replacement of the spear. The primary spear was designed to be easily replaceable in the event of the shear pin

breaking, and the latch mechanism enables easy detachment of the ghost pot from the ROV once at the surface, significantly reducing reset time between redeployments. Finally, extensive analysis and physical experimentation proved our system more than exceeded the 900 N loading requirement and any interesting moments that could be encountered during the retrieval, disentanglement, redeployment process.

VI. Integrated System

Pool Test

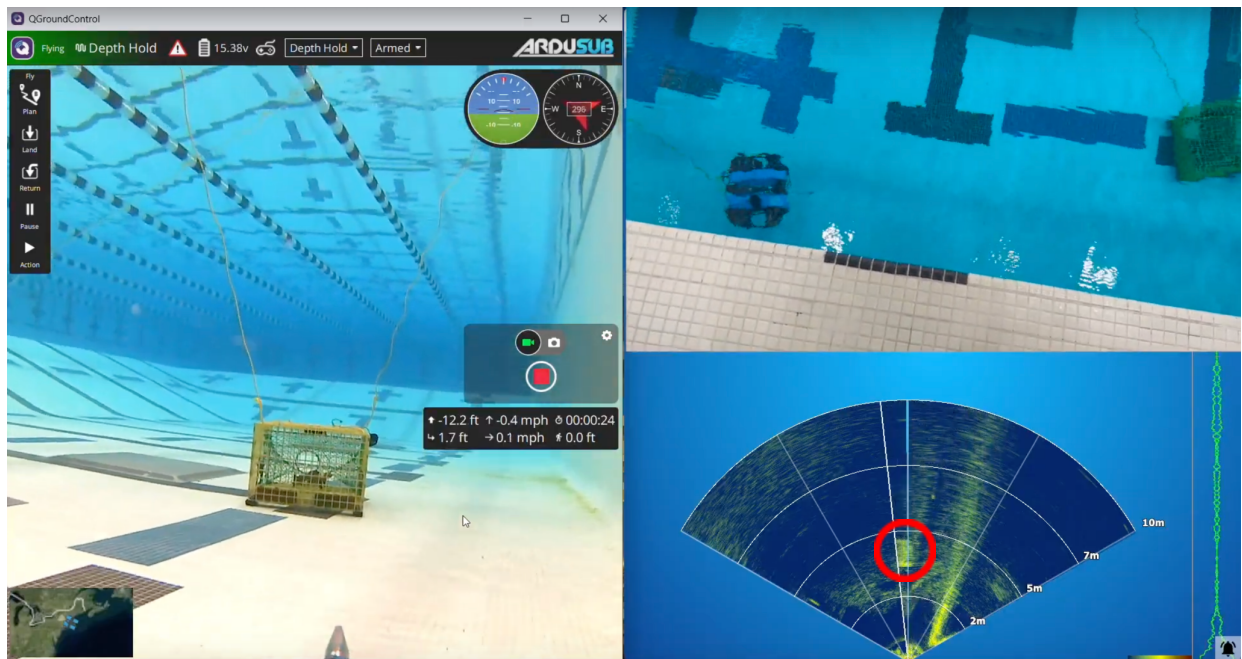


Fig. 35 Left: screenshot of video feed from ROV camera during pool test. Top: Overhead view of the ROV and pot during the pool test. Right: screenshot of ROV-mounted Ping 360 sonar view during the pool test with lobster pot circled in red.

For the pool test, we focused on determining the spear's ease of use and pot retrieval methodology. We set up a mock retrieval trial by dropping the lobster pot in a pool. Since the water was unoccluded, we used the onboard camera to navigate to the pot. We did confirm that the sonar was able to “see” the pot, but navigation was performed primarily with the camera for this test. From there, we speared the pot with ease and confirmed the engagement was secure.

Upon successful engagement, we hauled the pot out of the water by the ROV tether. We then disengaged the spear in order to detach the pot from the ROV. This process was repeated three times during which we varied the distance and bearing of the pot location as well as the initial depth and heading of our ROV. From this testing, we confirmed the viability of our pot retrieval method in ideal conditions.

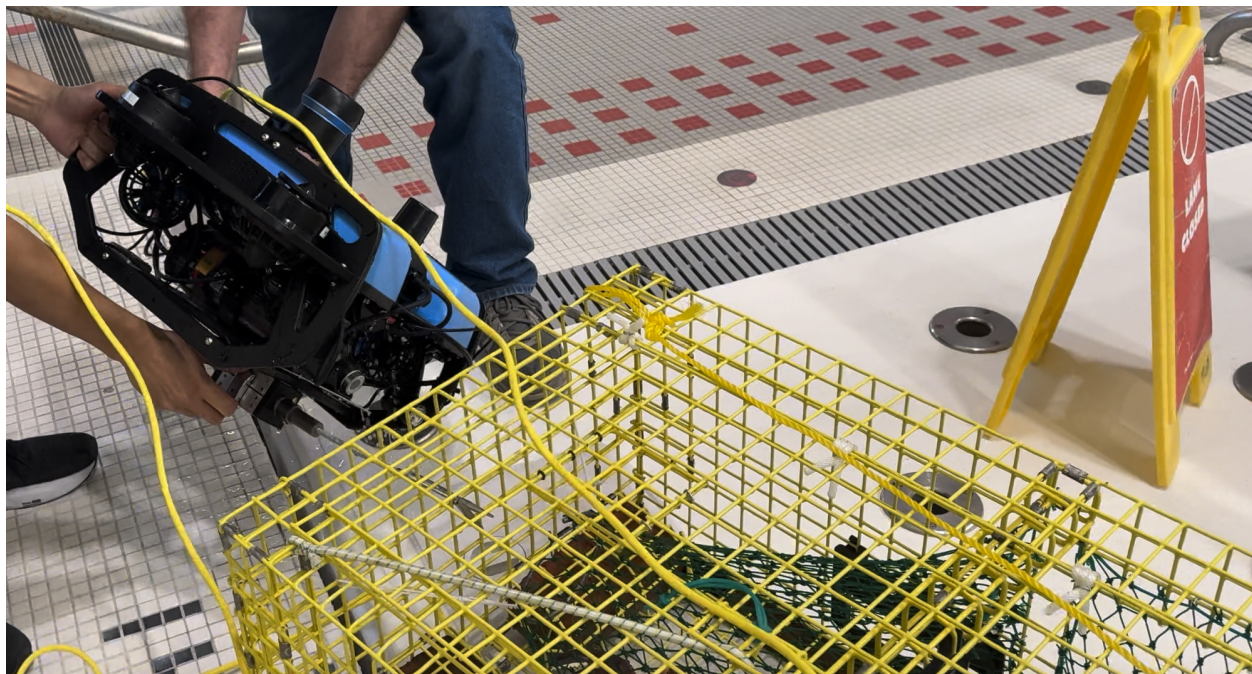


Fig. 36 ROV being pulled out of the indoor testing pool after successfully engaging the lobster pot.

River Test

For the river test, we wanted to confirm our methodology worked in less ideal conditions while also ensuring the viability of sonar based navigation. An additional worry was inexperienced operators, given this we had an untrained operator perform the following test. We set up a mock retrieval trial by throwing the lobster pot into the Charles River. We then dropped the ROV in and began the approach. Due to the current of the Charles River, manual navigation was not as simple as in the pool. We were able to successfully approach the pot by holding our

position while waiting for an update on the position of the pot from the sonar. At about one meter, the lobster pot became visible on the ROV camera (Fig. 11). Considering that the Charles River is highly turbid, we can expect increased performance in ocean conditions. Regardless, the sonar proved sufficient to navigate to the pot from fifteen meters away. In our initial spearing attempt, we missed the pot, but it was not difficult to make another pass, this time successfully. With successful engagement, we manually hauled in the line. From start to finish, we retrieved the pot in ten minutes using primarily sonar based navigation and an inexperienced operator, confirming the viability of our pot retrieval even in the worst case conditions: turbid with high current.



Fig. 37. Left: ROV camera view of the lobster pot in the Charles River. Right: Ping 360 sonar view of the lobster pot in the Charles River with lobster pot circled in red.

In addition to retrieval, one of our main focuses during testing was characterizing the ease of replacing the spear attachment in the event of breakaway. We determined that the swapping procedure was easy and likely could be performed with just a single hand.



Fig. 38. Left: spear in latch-box immediately after retrieval. Middle: spear being removed from latch box. Right: spear being removed from pot. Entire process completed in <12 seconds.

VII. Comparison to Current Solutions

Our ROV-based ghost pot retrieval system successfully bridges the existing value gap between lobster pot and crab pot retrieval. The full time, cost, and manpower comparison is presented in Table 2. Crucially, we find that ROV-based retrieval doubles the value of existing lobster pot retrieval efforts. This estimate accounts for the cost of the ROV system, system wear-and-tear, and volunteer availability. Retrieval time per pot was based on the ~10 minutes recorded during river testing plus travel time. The number of pots retrieved per day was estimated based on the typical length of one of the Cornell Cooperative Extension's expeditions—as reported in [7]. The retrieval cost per pot was calculated using the typical cost of a ghost pot retrieval expedition, as reported by UDel, and the additional cost of the ROV, divided by the expected number of pots retrieved over the course of two years. We estimate that, after more than two years, the cost in repairs due to wear and tear will be about equal to the cost of buying a new ROV.

Table 2. Retrieval Method Time and Cost Comparison

	Trawling (Lobster) [8]	ROV-Based Retrieval	Rope+ Grapple (Crab) ¹
Retrieval Time/Pot	~3.5 mins (17.5 mins/5 pots)	~2.5 min (12.5 mins/5 pots)	~16 mins
Retrieved Pots/Day	~67	~94	~50
Required # Ppl	2-3	2-3	2-3
Retrieval Cost/Pot	\$112***+ env. damage	\$84**	\$150
Market Value/Pot	\$202 [3] [7]	\$202 [3] [7]	\$800
Value Added/Day	\$6K	\$11.1K	\$32.5K

1. Based on emails with Professor Arthur Trembanis, University of Delaware School of Marine Science and Policy

We also assessed the viability of substituting an ROV-based retrieval system for current lineless lobstering methods. We found that ROV-based retrieval costs ~20% less than lineless lobstering, making it a desirable substitute. While our estimates indicate ROV-based retrieval is still more expensive than traditional lobstering, it is worth noting that an ROV-based system drastically reduces the risk of losing a pot, a risk exclusive to traditional lobstering methods that we do not account for when tabulating adjusted costs. Additionally, when calculating cost per pot for ROV-based retrieval, it is worth noting that ROV-based retrieval eliminates the need for highly regulated buoy lines that are engineered to break at specific loads to avoid entangling whales. While we do not have exact numbers on the cost of these specialized lines, we believe it is safe to assume that they likely make up a majority of the pot's price tag.

Table 3. Lobster Pot System Cost Comparison

	Line Less [7]	ROV-Based Retrieval	Traditional Method ¹
Fixed Cost/Pot	\$500 (\$2500/10 trawls)	\$100+\$147 (\$22000/1.5 yr)	\$100
Retrieval Time/Pot	1 min	~2 min	1 min
Deployed Pots/Day	250-300	~150	250-300
Adjusted Cost/Pot	\$500	\$412	\$100

1. Based on emails with Professor Arthur Trembanis, University of Delaware School of Marine Science and Policy

Finally, it's important to note that these analyses of ghost-pot retrieval and lineless lobstering go hand-in-hand. A lobsterman already equipped and practiced with an ROV-based system for retrieving his own lineless pots also has all the tools and skills necessary to retrieve ghost-pots in his area.

Taken independently, these analyses show that ROV-based lobster pot retrieval is a viable and competitive solution for both recovering ghost pots and lineless lobstering. Taken together, these analyses indicate that ROV-based retrieval is the best step towards deputizing lobstermen as ghost pot retrieval experts—and at last removing the literal millions of ghost pots that litter the ocean floor [5], [6].

VIII. Future Works

A. Localization

While we have made efforts to develop a robust localization methodology, we acknowledge there are improvements to be made that were not touched upon due to insufficient

time. A high priority for future work would be confirming the UDel system horizontal distance accuracy, as well as finding an estimate for depth accuracy. As such, we would be interested in performing tests in varied environments to confirm our use of the UDel sonar software in the real world system. A lower priority is testing USBL accuracy more thoroughly. Some examples of interest include: alternative environments, greater depth variation, drift over time testing and a general increase in samples per test for increased confidence in our conclusions. With these tests, we would be able to further confirm the viability of our testing setup and our intended real world use.

The localization team would also like to acknowledge the price component of our system. A combined DVL, USBL, Humminbird sonar and ROV system is expensive. While we would like to believe that the long term effectiveness increase is worth the upfront cost, it is an obstacle that we would prefer to avoid. Considering this, we would like to reduce the required system hardware for system localization to the minimum required for the desired effectiveness. We would need to engage in extensive testing to determine the ideal hardware reductions for the most effective price reductions.

B. Navigation

There are several improvements to the ROV's navigation system that could significantly decrease the time it takes to recover a pot. One of the most immediate and actionable changes is wrapping all control actions in a single executable program. Such a program would accept pot GPS location and output control action, allowing the ROV to autonomously swim to the pot's general location. This would remove the current need for a human to interface between UDel GPS coordinates, the boat's onboard GPS, and the set waypoint tool in QGroundControl. An additional improvement could involve either filtering the USBL signal or augmenting it with

data from the Humminbird to eliminate the necessity of the DVL. This would reduce the ROV's price by 33% or eight thousand dollars. Finally, a future version of the ROV that runs a version of UDel's pot detection software adapted to the ROV's Ping 360 sonar feed could enable fully autonomous approach and engagement—requiring human intervention only in the retrieval step.

C. Recovery

Mechanically, there are several improvements still to be made that could increase the longevity, reliability, and cost effectiveness of the design. The primary points for improvement are the barb, which was purchased off the shelf from a spear-fishing equipment manufacturer; the disengagement mechanism, which requires the barb to be left behind in the case that the ROV needs to disengage from the pot; and the latch-box, which is expensive to manufacture and heavy. We also intend to offer multiple shear pins and a stronger tether for lobstermen with stronger winches.

The current design for the barb is acceptable for our application because it fits the geometrical constraints of the overall system, and it is sufficiently strong such that the winch will stall before the barb breaks. However, under loads smaller than the design load, the current barb bends and deforms without failing, which can affect the usability of the system and require the barb to be replaced. The goal for the future is to develop and manufacture a barb that is specifically designed for the expected load conditions. This will extend the life span of the barb, allowing lobstermen to keep fewer replacement parts on hand and reducing the lifetime cost of the system.

Redesigning the barb could also include a solution to the current disengagement mechanism, which relies on leaving the barb behind with the lobster pot. This design, while operational, adds expense (roughly \$30 per lost spear), is a waste of materials, and leaves extra

waste on the ocean floor. For the future development of this system, we would like to revisit the sprung spear design or some other design that causes the barb to fold outwards under sufficiently large loads.

There are many reasons we did not develop this design for this stage of the project, however, most of them were time-constrained. The first issue with the design was the mathematical model we used to determine the point at which the prongs of the barb would bend outwards enough to disengage required springs with very specific characteristics be used. We were unable to find springs online with the exact spring constants, diameters, and total extension ranges we would need to make the system work. To solve for this in the future, custom springs will need to be ordered, which was not conducive to our timeline, or the system will need to be redesigned to accomplish the same effect while utilizing the springs differently.

How the springs are utilized to create the resistance on the opening barb also needs to be researched and developed. In our analysis, three types of springs were considered: torsional, which would cause the resistance to increase linearly with the barb prong angle, linear, which would cause the resistance to increase with the barb prong angle, but not linearly, and a constant force spring, which would initially increase the resistance with the barb prong angle, but would plateau at a certain point. The torsional and linear springs offer more longevity to the system and are easier to purchase, however, they limit the range of lobster pots that can be retrieved. For pots with finer mesh, the barbs need to bend outwards to a much larger angle than barbs with larger mesh.

The constant force springs, on the other hand, would support retrieving lobster pots of different sizes. For future development, it may be most effective to use these, however we encountered issues getting springs that were sufficiently strong, were reasonable sizes, and

would be corrosion resistant. This may be solvable by sheltering the springs in a separate part of the ROV and using a series of mechanical linkages to transfer the force, but this adds complexity to the system.

The next part of the spear assembly that could be improved is the latch-box in which the spear gets inserted to connect it to the ROV. The current design has eight screws, six non-fastener pieces, and the overall design is bulky and heavy. We believe, with a redesign, this part of the assembly could achieve the same effect with two to three non-fastener pieces, half as many screws, and an overall design that has less effect on the weight and dynamics of the system. Making this improvement would reduce manufacturing costs, improve reliability, and improve the ROV's battery life (by decreasing drag).

Finally, we are looking to conduct future tests to determine the overall strength of the system and create an accurate way to predict the load a given shear pin can support in our assembly. By confirming the maximum load our system can take and making improvements where necessary, we will be able to offer multiple shear pins to lobstermen with stronger winch systems on their vessels, allowing them to retrieve stubbornly stuck pots.

IX. Conclusions

The ROV system was able to manually navigate to a lobster pot, latch onto it, and be pulled back to the surface as demonstrated through pool and river testing. Although GPS waypoint navigation was not achieved, the USBL was able to show global positions that could be manually driven to. Within the short range navigation, onboard sonar and camera were sufficient to locate and latch onto the pot in water within one meter of visibility. The hooking mechanism

was able to consistently latch onto the lobster pot, with testing only requiring one to two attempts before latching.

Through testing, it was determined that the USBL system is able to track the live position of the ROV with roughly three meters of accuracy. However, as our tests were conducted in a highly reflective diving pool, it is possible that our positioning error may be lower in real-world conditions. Additionally, we validated that the USBL system sufficiently modeled the GPS coordinates given by the University of Delaware software. The discrepancy between the horizontal distance errors is minor enough that we are confident that the results from our testing environment will translate to real-world conditions.

With the testing of the USBL system and various navigation methods, the groundwork for autonomous navigation has been laid, though full implementation was limited by testing constraints. While the DVL can improve performance in murky conditions, it may not be necessary in clear water where USBL data is sufficient. Ultimately, reliable navigation depends on tuning and testing the system, including QGroundControl's PID parameters, in the actual deployment environment.

The retrieval mechanism has been verified to be successful and relatively easy to operate, both on the ROV and on deck, with a low manufacturing cost. While the current shear pin stress tests did not cause it to break at the desired forces, this can be addressed in future works by testing multiple shear pins with various thicknesses, configurations, or materials. Additionally, a stronger custom barb can be made for a longer lifespan, and the latch mechanism can be optimized as well. With additional time and resources, using a spring spear mechanism will likely be the first alternative design to be explored since it retains the advantages of the single

hook without the disadvantages of a break-off fuse mechanism, which would make the entire operation smoother and eliminate waste on the seabed.

The recovery time of the system was estimated at 10 minutes per cycle, which includes time to drive the boat to location and time to pull the ghost pot back to the surface. Compared to the UDel recovery time of 15 to 23 min in similar depth water to our testing conditions, the retrieval time is reduced, which increases efficiency in the retrieval process. The time could be further reduced with more autonomy integration. The ROV total cost amounted to around twenty-two thousand dollars, with the expectation that future iterations will cost less. The ROV cost is offset by the increased number of lobster pots retrieved over approximately four typical ghost pot recovery trips.

References

- [1] “Lobster Market Size, Share And Industry Report 2033.” Accessed: May 14, 2025. [Online]. Available: <https://www.imarcgroup.com/lobster-market>
- [2] “Fishing for Derelict Lobster Gear in Cape Cod and Massachusetts Bays | Marine Debris Program.” Accessed: May 14, 2025. [Online]. Available: <https://marinedebris.noaa.gov/removal/fishing-derelict-lobster-gear-cape-cod-and-massachusetts-bays>
- [3] “Lobster Price in US - May 2025 Market Prices (Updated Daily).” Accessed: May 14, 2025. [Online]. Available: <https://www.selinawamucii.com/insights/prices/united-states-of-america/lobster/>
- [4] N. H. Photography, “Ghost lobster trap, San Clemente Island, California, #30872.” Accessed: May 14, 2025. [Online]. Available: <https://www.oceanlight.com/spotlight.php?img=30872>
- [5] “Impact of ‘Ghost Fishing’ via Derelict Fishing Gear,” *NOAA Marine Debris Program*, p. 25, Mar. 2015.
- [6] “Gear Grab – GOMLF.” Accessed: May 07, 2025. [Online]. Available: <https://www.gomlf.org/gear-grab/>
- [7] G. Baggi, “Ghost Fishing Off Long Island’s Coast,” Undark Magazine. Accessed: May 14, 2025. [Online]. Available: <https://undark.org/2019/01/02/ghost-fishing-long-island-coast/>
- [8] N. Fisheries, “American Lobster | NOAA Fisheries,” NOAA. Accessed: May 14, 2025. [Online]. Available: <https://www.fisheries.noaa.gov/species/american-lobster>
- [9] “How to Go Crabbing with Pull Traps | FishTalk Magazine.” Accessed: May 14, 2025. [Online]. Available: <https://www.fishtalkmag.com/blog/how-go-crabbing-pull-traps>
- [10] N. Ogrysko, “These divers are trying to make a dent in Maine’s ‘ghost gear’ problem, one abandoned trap at a time.” Accessed: May 14, 2025. [Online]. Available: <https://www.wbur.org/news/2024/11/01/ghost-gear-lobster-traps-maine-gulf-clean-up>
- [11] “Project Gallery,” Kaitlyn Becker. Accessed: May 14, 2025. [Online]. Available: <https://kaitbecker.com/project-gallery>
- [12] “Guardian Ropeless Systems | Simple, Low-tech, and Affordable Ropeless Solutions,” Guardian Ropeless Systems. Accessed: May 14, 2025. [Online]. Available: <https://guardianropeless.com/>

